European Journal of Medicinal Chemistry xxx (2018) xxx-xxx

Contents lists available at ScienceDirect

European Journal of Medicinal Chemistry

journal homepage: www.elsevier.com

Research paper

Investigating alkyl nitrates as nitric oxide releasing precursors of multitarget acetylcholinesterase-monoamine oxidase B inhibitors

Leonardo Pisani[a, *], Rosa Maria Iacobazzi[b], Marco Catto[a], Mariagrazia Rullo[a], Roberta Farina[a], Nunzio Denora[a], Saverio Cellamare[a], Cosimo Damiano Altomare[a]

[a] *Dipartimento di Farmacia-Scienze del Farmaco, Università degli Studi di Bari "Aldo Moro", via E. Orabona 4, 70125, Bari, Italy*
[b] *Istituto Tumori IRCCS Giovanni Paolo II, viale O. Flacco 65, 70124, Bari, Italy*

ARTICLE INFO

Article history:
Received 30 July 2018
Received in revised form 4 October 2018
Accepted 8 October 2018
Available online xxx

Keywords:
Acetylcholinesterase
Monoamine oxidase B
Nitric oxide donor
Multitargeting agents

ABSTRACT

Herein we envisaged the possibility of exploiting alkyl nitrates as precursors of alcohol-bearing dual inhibitors targeting acetylcholinesterase (AChE) and monoamine oxidase B (MAO B), key enzymes in neurodegenerative syndromes such as Alzheimer's disease (AD), through biotransformation unmasking an alcoholic function upon nitric oxide (NO) release. The cooperation to neuroprotection of low fluxes of NO and target enzymes' inhibition by the alcohol metabolites might return a multitargeting effect. The in vitro screening towards ChEs and MAOs of a collection of 21 primary alcohols disclosed a subset of dual inhibitors, among which three diverse chemotypes were selected to study the corresponding nitrates. Nitrate **14** proved to be a brain permeant, potent AChE-MAO B inhibitor by itself. Moreover, it protected human SH-SY5Y lines against rotenone and hydrogen peroxide with a poor inherent cytotoxicity and showed a slow conversion profile to its alcohol metabolite **9d** that still behaved as bimodal and neuroprotective molecule.

1. Introduction

Alzheimer's disease (AD) is a devastating and ultimately fatal pathology [1] accounting for most of dementia cases worldwide. Giving that ageing is the main risk factor, the incidence of AD is expected to constantly mirror the increased life-expectancy. In addition, the cure for AD represents a health priority because of the lack of effective therapies [2,3]. Cognitive, motor and psychiatric deficits that impact daily-life activities appear as a consequence of dysfunctions in cerebral cortex areas mainly under cholinergic control [4,5]. Therefore, drugs able to restore appropriate neurotransmitter (namely acetylcholine, ACh) levels funded their rationale in the so-called cholinergic theory addressing the inhibition of ACh catabolic enzyme (acetylcholinesterase, AChE) [6]. Albeit merely palliative [7], AChE inhibitors are still the mainstay of AD treatment [8]. On the other side, the more recent amyloid hypothesis was related to the formation of senile plaques constituted by beta-amyloid (Aβ) peptide fibrils in AD brains [9]. Aβ deposits and neurofibrillary tangles (NFTs), formed by hyperphosphorylated tau protein, are the main hallmarks that led to the discovery of the most-validated AD biomarkers [10], whereas drug research programs addressing both mechanisms have failed so far in offering novel therapies [11].

Different abnormalities in neurons have been proved in AD brains, which include oxidative stress conditions [12] and reactive oxygen species (ROS) overloading [13], protein misfolding and deposition, unbalance in biometal concentrations [14], loss of synaptic function, inflammatory processes and many others [1], thus triggering the identification of several therapeutic options including insulin resistance [15] and lipid transport [16], too. However, none of the above-mentioned events has been clearly associated to the onset or to the relentless progression of the disease and, more importantly, all efforts have not resulted in new drugs on the market so far. In recent years, the multifactorial aetiology inspired the so-called multitarget strategy rooted on the idea that exploiting cooperative activities by multipotent molecules [17] could produce a more effective disease modifying action [18,19]. As a matter of fact, the latest innovative progression has been scored by a combination of two active ingredients each acting with a different mechanism [20], namely memantine (NMDA antagonist) and donepezil (AChE inhibitor).

In this context, dual-targeting compounds inhibiting AChE and monoamine oxidases (MAOs) have been reported by several authors [21–25]. AChE inhibition has been maintained as the core activity to

Abbreviations: ACh, acetylcholine; AChE, acetylcholinesterase; AD, Alzheimer's disease; BBB, blood brain barrier; BChE, butyrylcholinesterase; DIEA, *N*,*N*-diisopropylethylamine; DMEM, Dulbecco's modified eagle medium; ER, efflux ratio; FBS, fetal bovine serum; FD4, fluorescein isothiocyanate-dextran; GSH, glutathione; MAO, monoamine oxidase; MDCK, Madin-Darby Canine Kidney; MTT, 3-(4,5-dimethylthiazol-2-yl)-2,5-diphenyl-tetrazolium bromide; ND, neurodegenerative disease; NMDA, *N*-methyl-D-aspartate; NO, nitric oxide; P_{app}, apparent permeability; P_{app} AP, apparent permeability apical-to-basal; P_{app} BL, apparent permeability basal-to-apical; PBS, phosphate buffered saline; P-gp, P-glycoprotein; ROS, reactive oxygen species; RP-HPLC, reversed-phase high-performance liquid chromatography; SAR, structure-activity relationships; TEER, trans-epithelial electrical resistance; TLC, thin layer chromatography

* Corresponding author.
Email address: leonardo.pisani@uniba.it (L. Pisani)

https://doi.org/10.1016/j.ejmech.2018.10.016
0223-5234/

reduce central ACh deficits, whereas the inhibition of MAOs could potentially interfere with oxidative stress. In fact, MAO catalytic cycle produces hydrogen peroxide and its activity increases with ageing in both normal brains and in activated plaque-related astrocytes in AD [26]. As a follow-up of our recent contribution to the field of dual AChE-MAO B inhibitors [27,28],we devoted our efforts to add a third synergic activity to bimodal compounds that is the release of nitric oxide (NO). NO is a gaseous, endogenous, and rapidly diffusing messenger able to exert dose-dependent effects into the CNS [29]. High fluxes are cytotoxic since NO can react with superoxide anion, thus increasing peroxynitrite levels and consequent protein aberration upon nitration. In contrast, NO can work as neuroprotectant at low levels through *S*-nitrosylation of up-stream caspase-3 and activation of pro-survival pathways related to soluble guanylate cyclase (sGC). Up to date, the most explored therapeutic effect of NO is smooth muscle relaxation and, to this scope, several nitric oxide donors have been developed over the years [30]. More recently, nitrate hybrids have gained consensus in several therapeutic approaches, spanning from inflammation to anticancer therapies [31,32]. In most cases, they add a vasodilating effect to the core activity through a labile pendant moiety or a NO donor group. Since the metabolism of organic alkyl nitrates can release an alcoholic function [33], our idea was to explore whether selected alkyl nitrates can serve as precursors of alcohol bearing dual AChE-MAO B inhibitors upon nitric oxide release, thus working as multipotent small-molecule agents.

Organic nitrates lack a common degradation pathway in eukaryotes, and then a case-by-case study on different chemotypes is needed. On this basis, we initially developed a small collection of primary alcohols that were screened towards the target enzymes, namely acetyl- and butyrylcholinesterase (AChE and BChE) and monoamine oxidases (MAO A and B). The most promising inhibitors were then shortlisted to focused diverse samples and the corresponding nitrates were prepared and studied. The Griess assay along with the HPLC studies of nitrates stability in different experimental conditions (phosphate buffer at physiological pH with or without active thiols, namely cysteine and glutathione; human serum; cytosolic fraction from neuroblastoma cells) were undertaken to assess NO release and alcohol formation profile. Moreover, a preliminary investigation addressing cytotoxicity and neuroprotective action against oxidative insults (rotenone and H_2O_2) was carried out in human SH-SY5Y neuroblastoma cells. A cell-based model employing MDCKII-MDR1 cell lines was used to estimate the ability to cross blood-brain barrier (BBB) by the nitrates eligible for the desired alcohol metabolite release.

2. Design of alcohol probes

Diverse alcohol-based dual inhibitors were designed by combining three molecular bricks (Fig. 1), each carrying a potential pharmacodynamic feature, through different connection patterns: i) a basic and protonatable head was used to bind AChE anionic subsites [34–36]; ii) a planar coumarin scaffold to fit the MAO aromatic cage [37,38]; iii) a primary alcohol group as the structural element unmasked from the parent nitrate group after in vivo NO release. The decoration of the heterocyclic framework and the focused structural variations herein explored started from our previous studies highlighting two classes of dual AChE-MAO B coumarin-based inhibitors differing for the substitution at C7 (benzyloxy [27] and 1-piperidin-3(4)-yl-methoxy groups [28]) and for the multitarget profile. Taking advantage of previous extensive structure-activity relationships (SAR) developed for 7-benzyloxycoumarins, hindered substituents were avoided at position 4 [38] where a hydroxymethyl group greatly enhanced the dual activity. Unexplored positions 3 and 4 of 7-{piperidin-4-yl]methoxy}-2*H*-chromen-2-ones have been concerned by addressing the effect of methyl groups whereas spacer and alcohol chain lengths were investigated at position 7. The design aimed at probing primary alkyl and benzyl alcohol groups in both compound classes to allow the selection of different alcohol/nitrate chemotypes.

3. Methods

3.1. Chemistry

As shown in Scheme 1, the synthesis of alcohols **3a-b** and **6a-c** was accomplished by the benzylation of the suitable 7-hydroxycoumarin (**1**, **2b** or **4a-b**) followed by nucleophilic substitution with *N*,*N*-dimethylamine or 4-piperidinemethanol in THF. Scheme 2 illustrates the preparation of piperidine-bearing compounds that started from the common intermediates **8a-g** obtained upon removal of Boc-protecting group from **7a-g** in acidic environment by TFA. Subsequent alkylation with the appropriate benzyl halides or ω-chloro(bromo)-1-alcohols in refluxing acetonitrile gave access to *N*-benzylpiperidines **9a-i** and *N*-alkylpiperidines **12a-f**, respectively. Unprotected piperidine **8a** was reacted with 3-(chloromethyl)phenol in the presence of DIEA to afford phenol **10** that underwent final alkylation with 3-bromopropan-1-ol thus yielding derivative **11**.

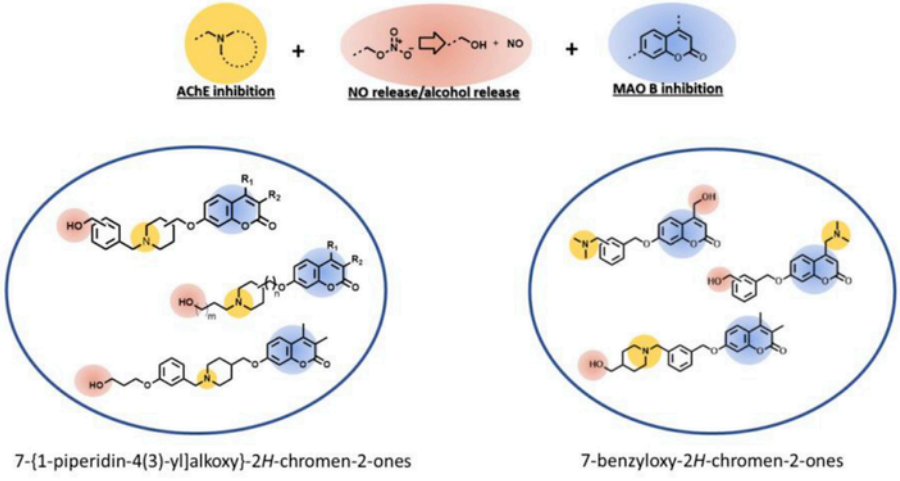

Fig. 1. Combination of molecular bricks to generate a collection of multipotent alcohols.

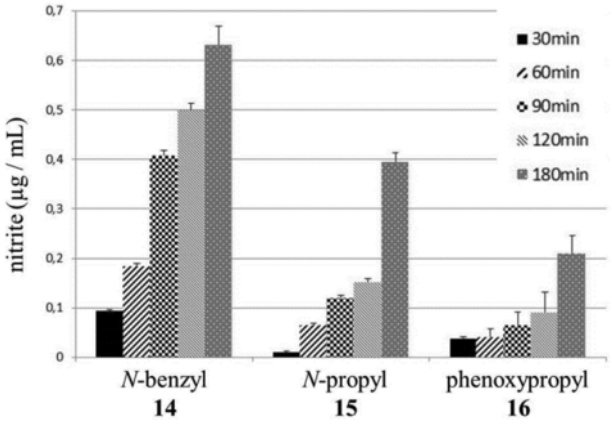

Fig. 2. NO release from nitrates **14–16** in the colorimetric Griess assay. The levels of NO_2^- ion (µm/mL) produced by compounds **14–16** (150 µM) were measured at different incubation time (30, 60, 90, 120, 180 min) with phosphate buffer (50 mM, pH = 7.40) containing cysteine (5 mM), before the addition of the Griess reagent. Calibration curve was derived from sodium nitrite standard solutions. Values are the mean ± SEM.

To prepare benzyl nitrate **14** (Scheme 3), intermediate **8a** was alkylated with α,α′-dichloro-*m*-xylene in acetone before transformation into **14** in the presence of silver nitrate in acetonitrile under reflux conditions. Conversely, nitrate esters **15** and **16** were prepared through a nucleophilic substitution employing **8a** or **10** and 3-bromopropyl nitrate [39], respectively.

3.2. Biological assays

Alcohol-bearing derivatives **3a-b**, **6a-c**, **9a-i**, **11**, **12a-f** and nitrates **14–16** were tested in vitro as inhibitors of human MAOs (hMAOs) and ChEs (eeAChE and esBChE) by applying a fluorescence-based protocol [27] and the well-established Ellman's spectrophotometric assay [40], respectively, to determine IC_{50}s on both isoforms. Human ChEs isoforms were applied on selected samples. The inhibition data are reported in Tables 1–4 as IC_{50} (µM) or as percentage of inhibition at 10 µM for the less active compounds.

NO release and alcohol release profiles were estimated to advance nitrates towards biological studies addressing cytotoxicity and neuroprotection. 3-(4,5-Dimethylthiazol-2-yl)-2,5-diphenyltetrazolium bromide (MTT) assay [41] was used to measure the percentage of viable human neuroblastoma SH-SY5Y cells referred to control experiment and determine both the cytotoxic effect of compounds **9d**, **12a**, **14–15** (Table 5) and their protective effect when co-incubated with two oxidative insults (hydrogen peroxide and rotenone) as illustrated in Fig. 8. Neuroprotection effects were compared to that of donepezil as standard marketed anti-Alzheimer's drug.

As previously reported [27], cell-based bidirectional transport studies were aimed at estimating the potential BBB permeation of compounds **9d**, **12a**, **14–15**, by measuring apical to basolateral (AP) and basolateral to apical (BL) apparent permeability (P_{app}) in Madin-Darby Canine Kidney (MDCK) cells. P_{app} (in units of cm/s) and efflux ratio (ER) were calculated and listed in Table 5.

4. Results and discussion

4.1. SAR and diverse alcohol probes identification

For the sake of convenience in SAR discussion, all the compounds tested on enzymatic targets (MAOs and ChEs) were grouped into three small congeneric subsets. Concerning MAOs, B/A selectivity was desirable to avoid cheese-effect drawbacks [42,43]. On the other side, several lines of evidence indicated the activity of BChE within AD brains as an attractive feature [44–46] thus the lack of ChEs isoform selectivity was not considered a major drawback. Looking at the benzyloxycoumarins **3a-b** and **6a-c**, the best results towards MAO B were obtained by installing the primary alcoholic function at the position 4 of the heterocyclic core and the basic nitrogen on the 7-benzyloxy group. The smallest basic chain was tolerated at both *meta*- and *para*-position of the phenyl ring, giving rise to selective MAO B inhibitors resulting much more potent than the "flipped" analogues where the basic and alcohol groups linkage positions are inverted (**6a** vs. **3a**, IC_{50} = 0.078 and 0.63 µM, respectively; **6b** vs. **3b**, IC_{50} = 0.054 and 1.1 µM, respectively). Unfortunately, an opposite trend was observed for AChE affinity (**3a** > **6a**, **3b** > **6b**), even so in the micromolar range. BChE affinity was quite low and improved by branching the benzyloxy group with a bulkier alcohol-bearing protonatable head (**6c**).

Within *N*-benzylpiperidines (**9a-i**, **11**), 1,4-piperidine ramification slightly enhanced MAO B inhibition unrelated to *m*- or *p*-phenyl substitution (**9c** > **9a** and **9d** > **9b**) without affecting AChE affinity to a great extent. A molecule belonging to this subset (**9c**) showed the highest potency towards MAO B of the whole series with IC_{50} equal to 0.029 µM along with a good B/A selectivity (SI = 48). An interesting effect could be ascribed to the methyl groups at C3 and C4 of the coumarin ring. Indeed, both groups were essential for dual activity and 4-methyl scored better binding interactions than 3-methyl towards both MAO B and AChE (**9c** > **9e** > **9g**; **9d** > **9f** > **9h**). The ho-

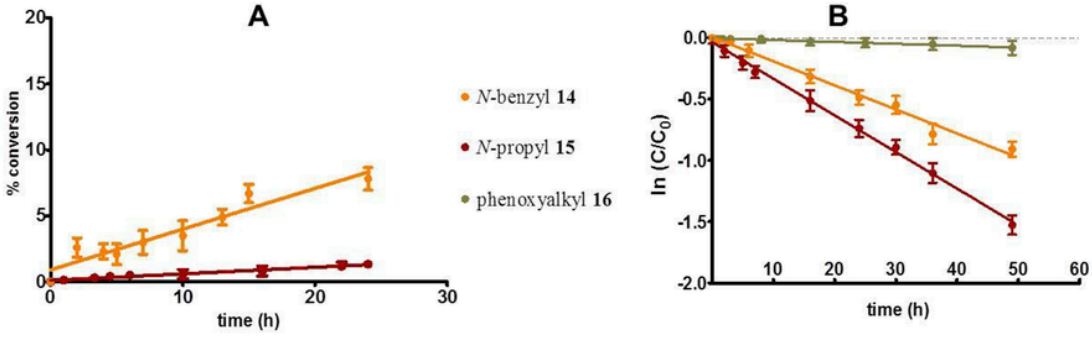

Fig. 3. Diagram of hydrolytic conversion to alcohol (A) and human serum stability plots (B) for nitrates **14–16**. Time-dependent formation of alcohols **9d** (orange plot) and **12a** (red plot) from **14** and **15**, respectively, was measured under hydrolytic conditions (A) in phosphate buffer (50 mM, pH 7.40, 0.20 M KCl) at 37 °C. Time-dependent disappearance of nitrates **14–16** was studied in human serum (B) at 37 °C. Compounds **14–16** were incubated at initial concentration equal to 100 µM and concentration at various time points was determined by RP-HPLC. Data points represent means ± SD of three independent measurements. (For interpretation of the references to color in this figure legend, the reader is referred to the Web version of this article.)

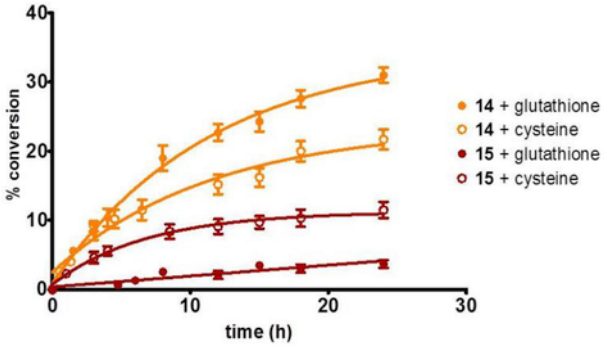

Fig. 4. Release profiles of alcohols **9d** (orange diagram) and **12a** (red diagram) from nitrates **14** and **15**, respectively, in the presence of thiols. Time-dependent formation of alcohols **9d** (orange) and **12a** (red) from nitrates **14** and **15**, respectively, was determined in phosphate buffer (50 mM, pH 7.40, 0.20 M KCl) containing 1 mM cysteine (○) or 1 mM glutathione (●) at 37 °C as determined by RP-HPLC. Nitrates **14**–**15** were incubated at initial concentration equal to 100 μM. Data are means ± SD of three independent assays. (For interpretation of the references to color in this figure legend, the reader is referred to the Web version of this article.)

mologation of the alcohol chain from **9c** to **9i** worsened mainly MAO B targeting activity. It is worth noting that a longer terminal chain (**11**) at position *meta* of the phenyl ring was able to revert selectivity (SI = 0.70 and 0.10 for MAO B/A and AChE/BChE, respectively) leading to a potent dual MAO A (IC_{50} = 0.55 μM) and BChE inhibitor (IC_{50} = 0.18 μM).

The third series includes *N*-alkylpiperidines **12a-f**, where the structural exploration addressed methyl groups on the coumarin ring, piperidine ramification pattern and linker length. As previously noticed, the 3,4-dimethyl substitution on the heterocyclic nucleus is a key player for the multitargeting activity (i.e., MAO B and AChE), as can be inferred by comparing **12a** vs. **12b** and **12e** vs. **12f**. 1,4-Piperidine substitution pattern performed a more efficient fit within MAO B enzymatic cleft than 1,3-ramification (**12a** > **12e**, **12b** > **12f**). Interestingly, the length of the spacer connecting coumarin to piperidine ring proved to be crucial for MAO B affinity since its homologation drastically dropped down the potency of **12d** compared to **12a** (IC_{50} > 10 μM and IC_{50} = 0.48 μM, respectively), while increasing AChE affinity (**12d**, IC_{50} = 0.72 μM; **12a**, IC_{50} = 1.3 μM). A similar effect resulted from the alkyl chain elongation within the terminal N-substituent, therefore butanol-derivative **12c** showed a detrimental MAO B affinity (IC_{50} = 3.6 μM) along with an improved AChE inhibition (IC_{50} = 0.50 μM) compared to propanol-derivative **12a**.

After clustering the alcohols in three subsets (Figure S1 in Supporting Information: benzyl alcohols, alkyl alcohols bearing a *N*-alkyl basic head, alkyl alcohols bearing a *N*-benzyl basic head), we selected one sample from each group (**9d**, **11**, **12a**) to study diverse possible chemotypes: i) benzyl nitrate **14** (from **9d**); ii) *N*-propyl nitrate **15** (from **12a**); iii) phenoxypropyl nitrate **16** (from **11**). Within the most potent dual benzyl alcohols showing nanomolar MAO B inhibition potency along with low micromolar AChE affinity (**3a-b**, **6a-b**, **9a-h**), **9d** was preferred to the equipotent, yet chiral, analogue **9a** and to *para*-substituted congener **9c** in order to circumvent solubility issues, more likely detectable with symmetric compounds [28]. Nitrate **15**, deriving from *N*-propyl alcohol **12a**, was chosen to probe compounds with both alkyl alcohols and alkyl basic nitrogen (**12a-f**) since it displayed the best multitarget profile. The study encompassed also phenoxyalkyl nitrate **16**, showing an interesting pan-inhibitor profile related to alcohol **11**. The corresponding nitrates were synthesized according to Scheme 3, tested in vitro against target enzymes, and their stability and NO-release, as well as the alcohol formation profile, were investigated in different experimental conditions.

4.2. In vitro assays for nitrates: NO-release and target enzymes' inhibition

The colorimetric quantitation of the azo-dye formed in the Griess assay was employed to measure NO release [47]. As inferred from Fig. 2, all compounds behaved as NO-donors and a time-dependent release was performed in all cases with the benzyl chemotype **14** providing the highest nitrite yields.

In vitro biological evaluation towards human target enzymes was extended to nitrates **14**–**16**. Data are reported in Table 4 compared to alcohols, which showed that the nitrate group was well-tolerated by both hMAO B and hAChE. More importantly, it enhanced MAO B affinity in all cases compared to the alcohol product (**14** > **9d**, **15** > **12a**, **16** > **11**) and originated potent inhibitors in the nanomolar range. Non-homogeneous clues could be gathered about the other targets, where the presence of nitrate promoted different affinity performances.

4.3. RP-HPLC study of nitrate-alcohol conversion profiles

In vivo nitrate decomposition can occur via hydrolysis or reductive denitration. However, no specific enzymatic pathway is available in eukaryotes because of the absence of specific hydrolases acting on nitrates. Importantly, hydrolytic by-products include chemical species different from the putative alcohol that might originate from elimination (α-H, β-H) or nucleophilic substitution reactions (e.g., alkene,

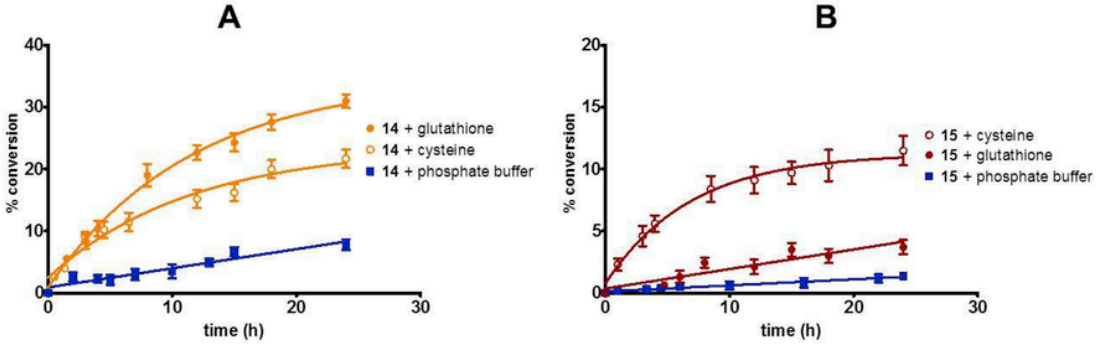

Fig. 5. Conversion rates of *N*-benzyl nitrate **14** (A) and *N*-propyl nitrate **15** (B) in different conditions. Time-dependent formation of alcohols **9d** (A) and **12a** (B) from nitrates **14** (100 μM) and **15** (100 μM), respectively, was determined in phosphate buffer (50 mM, pH 7.40, 0.20 M KCl) containing 1 mM cysteine (○) or 1 mM glutathione (●) and compared to thiol-free phosphate buffer (blue) at 37 °C as determined by RP-HPLC. Data are means ± SD of three independent assays. (For interpretation of the references to color in this figure legend, the reader is referred to the Web version of this article.)

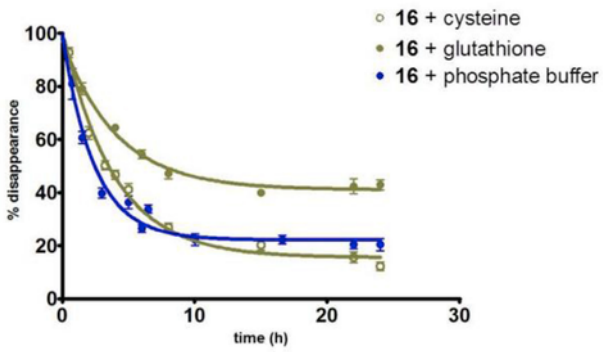

Fig. 6. Decomposition rate of nitrate **16** in different conditions. Time-dependent disappearance of compound **16** (100 μM) was measured at 37 °C in phosphate buffer (50 mM, pH 7.40, 0.20 M KCl) with 1 mM cysteine (○, green) or 1 mM glutathione (●, green) and without thiols (●, blue). The ratio between concentrations at various time points (C) and the initial concentration at t_0 (C_0) was determined by RP-HPLC. Data points represent means ± SD of three independent measurements. (For interpretation of the references to color in this figure legend, the reader is referred to the Web version of this article.)

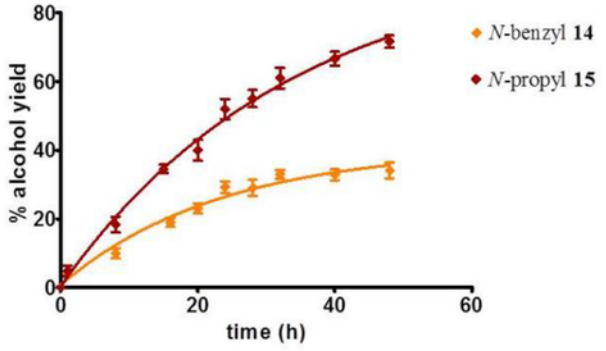

Fig. 7. Alcohol formation profiles from nitrates **14**–**15** in cellular environment. Time-dependent formation of alcohols **9d** (orange) and **12a** (red) from nitrates **14** and **15**, respectively, both incubated (50 μM) at 37 °C in cytosolic fractions of human SH-SY5Y neuroblastoma cells, as determined by RP-HPLC. Data represent triplicates' means ± SD. (For interpretation of the references to color in this figure legend, the reader is referred to the Web version of this article.)

aldehyde), which could in principle decrease alcohol release rate and yield.

The RP-HPLC method enabled to check the parent nitrates stability and their conversion rate to the alcohol metabolites in phosphate buffer at pH 7.40 and in human serum (Fig. 3). At physiological pH (Fig. 3A), about 7% of **9d** was retrieved from **14** and trace alcohol **12a** from **15** after 24 h incubation, suggesting that non-enzymatic hydrolysis at physiological pH does not play any role in the biotransformation of these nitrates into the alcohol product. Levels of alcohol **11** (data not shown) under the limit of detection were formed from **16**. In human serum, all three candidates exhibited a degradation profile that followed pseudo-first order kinetics and displayed an outstanding stability ($t_{1/2}$ = 23 h, 36.8 h, 458 h for **15**, **14** and **16** respectively) without releasing appreciable amounts of alcohols. In fact, a conversion yield to alcohol lower than 5% was retrieved in all cases after 48 h.

Apart from non-enzymatic degradation, we considered intriguing to investigate the reactivity towards reductive denitration pathways. This type of cleavage might be catalyzed in vivo by hemoproteins (iron-promoted) and active thiols (cytosolic and microsomal glutathione-*S*-transferases, GST, and glutathione, GSH), in both cases releasing NO and alcohol by-product [33].

As a preliminary examination, the susceptibility towards reductive cleavage promoted by active thiols was studied by adding an excess of cysteine or GSH to degassed phosphate buffer and by applying a 24 h co-incubation window in order to limit background disulfide formation. By monitoring the nitrate disappearance and the formation of the alcohol product, a RP-HPLC protocol was applied to estimate the stability of parent nitrates in the presence of free thiols and to predict the possible transformation from nitrate to primary alcohol metabolites along with inherent NO release in vivo. As for *N*-benzyl derivative **14**, GSH boosted the conversion from parent nitrate and showed a higher conversion rate compared to cysteine (Fig. 4). An opposite scale and an attenuated reactivity were observed in the case of the *N*-propyl chemotype **15** that behaved as a quite poor donor with low alcohol formation as illustrated by red plots in Fig. 4.

As a trend, plots in Fig. 5 indicate potentiating effects of thiols enabling higher alcohol yields and rates from **14** and **15** compared to hydrolysis in phosphate buffer at pH 7.40 (blue lines).

In the case of the phenoxypropyl chemotype **16**, no appreciable level of alcohol **11** was detected up to 24 h with and without thiols. However, this low release could not be ascribed to the nitrate stability in the experimental conditions. As can be inferred from the graph in Fig. 6, the disappearance of parent nitrate **16** proceeded rapidly, consuming more than 50% after 24 h in all experiments. Therefore, unwanted degradation by-products were formed, which ruled out the desired biotransformation into alcohol **11** and this sample was excluded from subsequent assays.

We further probed the behaviour in a cellular environment of the two chemotypes (**14** and **15**) enabling thiol-mediated alcohol release (Fig. 7). The stability and conversion profiles were assessed in the freshly prepared cytosolic fractions of human neuroblastoma cell lines. Both nitrates disclosed a retard-release profile and **15** exhibited higher alcohol yield than **14** (52% and 71% for **15**, 31% and 34% for **14** after 24 h and 48 h, respectively). The slow conversion rate may prefigure low NO fluxes in vivo, which could shift the bioactivity balance towards neuroprotection.

4.4. Cell-based studies

The ability of compounds to protect neurons from oxidative damage is a critical feature for anti-AD candidates. In the human neuroblastoma SH-SY5Y cell-based protocol [48], only the nitrates enabling alcohol release (**14** and **15**) were co-incubated at different concentrations (2.5, 0.5 and 0.1 μM) with two pro-oxidant toxins (rotenone at 20 μM and hydrogen peroxide at 200 μM). Cell viability was measured through MTT-assay [41]. Untreated cells were used as control and donepezil was taken as the reference compound. For comparative purposes, the respective alcohol metabolites **9d** and **12a** were engaged in the assays.

As shown in Fig. 8, all tested compounds (parent nitrates **14**, **15** and alcohols **9d**, **12a**) showed a dose-dependent inverse correlation with neuroprotection against cytotoxic insults, and the percentage of viable cells increased to a greater extent with the lowest concentration (0.1 μM). Interestingly, comparable figures of neuroprotection were obtained for nitrate **14** and donepezil with the exception of the highest concentration (2.5 μM) against rotenone when viability increase with donepezil was by far superior. In all experiments with nitrate ester **14**, the percentage of viable cells relative to control was higher or quite close to its putative metabolite **9d**. In particular, a greater viability gain than **9d** was observed when **14** was co-incubated at 0.5 and 0.1 μM concentrations with rotenone and at 2.5 μM concentration in the presence of hydrogen peroxide. An opposite trend was returned by *N*-propyl chemotypes (**15** and **12a**), thus alcohol **12a** protected SH-SY5Y neurons from both toxins more efficiently or closely to NO-donor **15** at all doses.

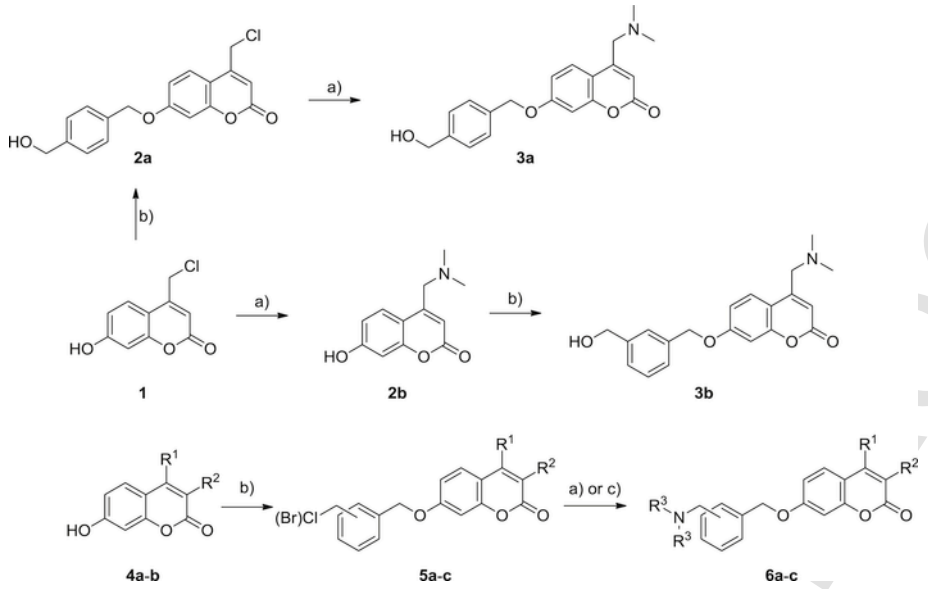

Scheme 1. Synthesis of compounds **3a-b** and **6a-c**[a] [a] Reagents and conditions: a) for **2b**, **3a**, **6a**–**b**: 2.0 N solution of *N*,*N*-dimethylamine in THF, room temperature, dry THF, 6 h; b) suitable benzyl chloride or bromide, K_2CO_3, dry acetonitrile, reflux, 1–8 h; c) for **6c**: 4-piperidinemethanol, DIEA, dry acetone, room temperature, overnight.

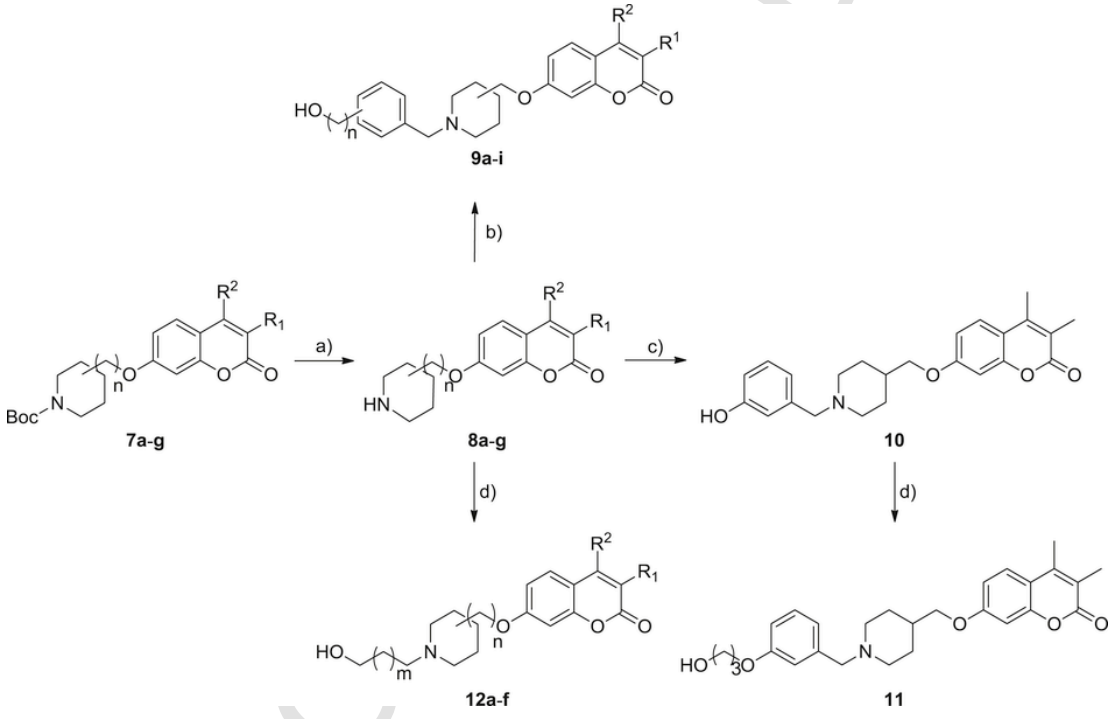

Scheme 2. Synthesis of compounds **9a-i**, **11**, and **12a-f**[a] [a] Reagents and conditions: a) TFA, dry CH_2Cl_2, room temperature, overnight; b) [3- or [4-(chloromethyl)-phenyl]methanol, K_2CO_3, KI (cat.), dry acetonitrile, reflux, 6 h (for **9a-h**) or 2-[4-(bromomethyl)phenyl]ethanol, DIEA, dry acetone, room temperature, 15 h (for **9i**); c) 3-(chloromethyl)phenol, DIEA, dry acetone, room temperature, 7 h; d) 3-bromopropan-1-ol (for **11**, **12a-b**, **12d-f**) or 4-chlorobutan-1-ol (for **12c**), K_2CO_3, KI, dry acetonitrile (for **12a-f**) or dry acetone (for **11**), reflux, 4–8 h.

In addition, the same cell line was used to assess the cytotoxicity of compounds **9d**, **12a**, **14** and **15** at concentrations ranging from 100 to 0.01 μM. As indicated by data in Table 5, **9d** and the respective parent nitrate **14** produced a low cellular damage (IC_{50} = 42.9 and 35.5 μM, respectively) whereas both **12a** and **15** were much less cytotoxic (IC_{50} > 100 μM).

To endorse the potential as CNS drugs, an in vitro blood-brain barrier penetration model was employed to study the bidirectional transport across MDCKII-MDR1 cells and predict CNS permeation [49]. Moreover, this protocol provides a reliable evaluation of the chance that xenobiotics are pumped out by P-glycoprotein (P-gp), which prevents central bioactivity. Both alcohols (**9d**, **12a**) and nitrate **14** might penetrate into CNS through passive diffusion with permeability comparable to diazepam and without interactions with efflux system (ER < 2). Unfortunately, *N*-propyl compound **15** seems to

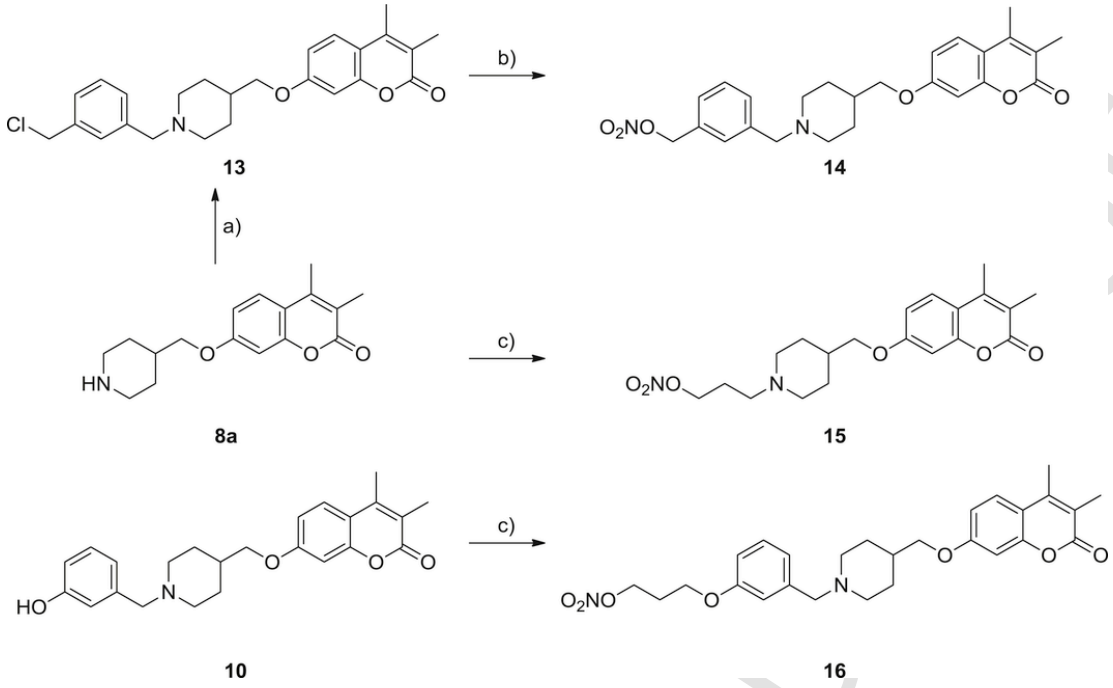

Scheme 3. Synthesis of nitrates **14**–**16**[aa] Reagents and conditions: a) α,α′-dichloro-*m*-xylene, DIEA, dry acetone, room temperature, 15 h; b) $AgNO_3$, dry acetonitrile, reflux, 6 h; c) 3-bromopropyl nitrate, K_2CO_3, dry acetonitrile, room temperature (24 h, for **15**) or reflux (4 h, for **16**).

Table 1

MAOs and ChEs inhibition data for alcohols **3a-b**, **6a-c**.

compd	R^1	R^2	R^3	IC_{50} (μM) or % inhibition at 10 μM[a]			
				MAO A[b]	MAO B[b]	AChE[c]	BChE[d]
3a	H	$CH_2N(CH_3)_2$	*p*-CH_2OH	23 ± 1.0%	0.63 ± 0.12	1.3 ± 0.020	11 ± 1.6
3b	H	$CH_2N(CH_3)_2$	*m*-CH_2OH	21 ± 3.2%	1.1 ± 0.11	4.4 ± 1.0	35 ± 2.2%
6a	H	CH_2OH	*p*-$CH_2N(CH_3)_2$	20 ± 3.4%	0.078 ± 0.013	4.5 ± 0.52	43 ± 1.1%
6b	H	CH_2OH	*m*-$CH_2N(CH_3)_2$	42 ± 2.9%	0.054 ± 0.0050	5.9 ± 0.61	36 ± 1.4%
6c	CH_3	CH_3	*m*-[4-(CH_2OH) piperidin-1-yl]	23 ± 1.3%	0.32 ± 0.12	2.9 ± 0.43	1.0 ± 0.040
safinamide				20 ± 3.0%	0.018 ± 0.0030		
clorgyline				0.0038 ± 0.00050	2.5 ± 0.43		
donepezil						0.024 ± 0.0040	2.1 ± 0.22

[a] Values are the means of three independent experiments.

[b] Human recombinant MAOs.

[c] AChE from electric eel.

[d] BChE from equine serum.

suffer from P-gp liability, which could hamper its further development.

5. Conclusions

In this study, we aimed at finding multitargeting organic nitrates that can serve as precursors of alcohol bearing dual AChE-MAO B inhibitors after biotransformation that can be non-enzymatically promoted by active thiols (e.g., glutathione). We initially focused our attention to the development of the active metabolites, namely alcohol-bearing dual AChE-MAO B inhibitors. Then, by applying a structural diversity filter, we fished three samples out the most potent alcohols (**9d**, **12a**, **11**) to study the corresponding nitrates. In the RP-HPLC study, the three nitrates displayed outstanding stability at physiological pH and in human serum, without releasing the alcohol product. All of them proved to be potent in vitro MAO B inhibitors, stronger than the putative alcohol metabolites. In the presence of bioactive thiols, two different NO donors (**14**–**15**) might work as co-drugs of alcohol-based bimodal AChE-MAO B inhibitors. In particular, we identified a brain permeant and serum stable nitrate (i.e., the *N*-benzyl chemotype **14**) able to perform a slow NO release and to yield good amount of the suitable primary alcohol (**9d**) in the presence of GSH as well as in cytosolic preparations of SH-SY5Y human neuroblastoma cells. Therefore, compound **14** should deserve further attention since it behaved as a multipotent molecule by itself (MAO B IC_{50} = 0.051 μM, AChE IC_{50} = 1.6 μM) and as a multitargeting precursor for a still active dual inhibitor (namely the alcohol metabolite **9d**, IC_{50} = 0.076 and 1.0 μM towards MAO B and AChE, respectively) upon NO release. Both parent NO-donor and the related alcohol ex-

Table 2

MAOs and ChEs inhibition data for alcohols **9a-i**, **11**.

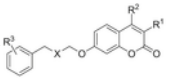

compd	R^1	R^2	X	R^3	IC_{50} (μM) or % inhibition at 10 μM[a]			
					MAO A[b]	MAO B[b]	AChE[c]	BChE[d]
9a	CH_3	CH_3		*p*-CH_2OH	1.1±0.20	0.076±0.010	1.2±0.020	8.6±0.050
9b	CH_3	CH_3		*m*-CH_2OH	2.2±0.10	0.11±0.015	0.90±0.080	2.7±0.28
9c	CH_3	CH_3		*p*-CH_2OH	1.4±0.30	0.029±0.0080	1.0±0.070	8.8±1.4
9d	CH_3	CH_3		*m*-CH_2OH	1.9±0.060	0.076±0.0080	1.0±0.040	1.3±0.12
9e	H	CH_3		*p*-CH_2OH	11±1.5	0.60±0.064	1.6±0.33	45±3.4%
9f	H	CH_3		*m*-CH_2OH	3.5±0.040	0.48±0.081	1.6±0.11	1.9±0.21
9g	CH_3	H		*p*-CH_2OH	43±5.2%	3.1±0.047	3.0±0.30	8.1±0.34
9h	CH_3	H		*m*-CH_2OH	3.9±0.81	1.1±0.034	3.2±0.37	0.91±0.19
9i	CH_3	CH_3		*p*-CH_2CH_2OH	1.7±0.17	0.12±0.020	1.2±0.22	41±7.3%
11	CH_3	CH_3		*m*-$O(CH_2)_3OH$	0.55±0.038	0.78±0.050	1.8±0.32	0.18±0.020

[a] Values are the means of three independent experiments.

[b] Human recombinant MAOs.

[c] AChE from electric eel.

[d] BChE from equine serum.

Table 3

MAOs and ChEs inhibition data for alcohols **12a-f**.

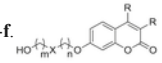

compd	R	X	n	m	IC_{50} (μM) or % inhibition at 10 μM[a]			
					MAO A[b]	MAO B[b]	AChE[c]	BChE[d]
12a	CH_3	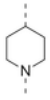	1	1	44±5.2%	0.48±0.050	1.3±0.040	30±3.1%
12b	H		1	1	26±4.4%	48±1.1%	38±2.3%	26±2.4%
12c	CH_3		1	2	30±4.1%	3.6±0.24	0.50±0.020	8.3±1.2
12d	CH_3		2	1	35±3.2%	31±3.1%	0.72±0.097	39±4.4%
12e	CH_3		1	1	41±3.0%	1.5±0.13	1.8±0.060	26±3.2%
12f	H		1	1	14±3.3%	42±1.0%	3.5±0.82	1.7±0.76

[a] Values are the means of three independent experiments.

[b] Human recombinant MAOs.

[c] AChE from electric eel.

[d] BChE from equine serum.

hibited significant neuroprotective activities against the pro-oxidative insults rotenone and H_2O_2 without producing cytotoxic effect in human neuroblastoma cell lines.

6. Experimental section

6.1. Chemistry

Starting materials, reagents, and analytical grade solvents were purchased from Sigma-Aldrich (Europe). The purity of all the intermediates, checked by HPLC, was always better than 95%. All the newly prepared and tested compounds showed purity higher than 95% (elemental analysis). Elemental analyses were performed on the EuroEA 3000 analyzer only on the final compounds tested as MAOs and ChEs inhibitors. The measured values for C, H, and N agreed to within ±0.40% of the theoretical values. Column chromatography was performed using Merck silica gel 60 (0.063–0.200 mm, 70–230 mesh). All reactions were routinely checked by TLC using Merck Kieselgel 60 F_{254} aluminum plates and visualized by UV light or iodine. Regarding the reaction requiring the use of dry solvents, the glassware was flame-dried and then cooled under a stream of dry argon before the use. Nuclear magnetic resonance spectra were recorded on a Varian Mercury 300 instrument (at 300 MHz) or on an Agilent Technologies 500 apparatus (at 500 MHz) at ambient temperature in the specified deuterated solvent. Chemical shifts (δ) are quoted in parts per million (ppm) and are referenced to the residual solvent peak. The coupling constants *J* are given in Hertz (Hz). The following abbreviations were used: s (singlet), d (doublet), dd (doublet of doublet), t (triplet), q (quadruplet), qn (quintuplet), m (multiplet), br s (broad signal); signals due to OH and NH protons were located by deuterium exchange with D_2O. The attribution of ^1H NMR signals was supported by comparison with gHSQC experiments carried out for selected samples (**9b**, **9c**, **11**, **12e**) as reported in Supporting Information. HRMS experiments were performed with a dual electrospray interface (ESI) and a quadrupole time-of-flight mass spectrometer (Q-TOF, Agilent 6530 Series Accurate-Mass Quadrupole Time-of-Flight LC/MS, Agilent Technologies Italia S.p.A., Cer-

Table 4

hMAOs and hChEs inhibition data for alcohols **9d**, **12a**, **11**, and corresponding nitrates **14**–**16**.

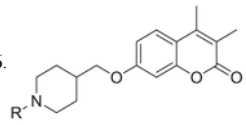

compd	R	IC_{50} (μM) or % inhibition at 10 μM[a]			
		MAO A[b]	MAO B[b]	AChE[c]	BChE[d]
14	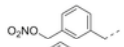	0.23 ± 0.0080	0.051 ± 0.0050	1.3 ± 0.27	n.t.[e]
9d	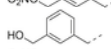	1.9 ± 0.060	0.076 ± 0.0080	1.4 ± 0.21	n.t.[e]
15		36 ± 2.2%	0.25 ± 0.068	0.86 ± 0.040	<5%
12a		44 ± 5.2%	0.48 ± 0.050	0.89 ± 0.12	<5%
16	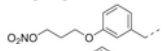	1.2 ± 0.12	0.55 ± 0.038	0.48 ± 0.041	0.80 ± 0.14
11	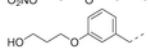	0.55 ± 0.038	0.78 ± 0.050	0.84 ± 0.11	0.74 ± 0.013

[a] Values are the means of three independent experiments.

[b] Human recombinant MAOs.

[c] Human recombinant AChE.

[d] BChE from human serum.

[e] n.t. = not tested.

Table 5
Cytotoxicity and bidirectional transport across MDCKII-MDR1 cells of nitrates **14**–**15** and alcohols **9d**, **12a**.

compd	Cytotoxicity[a]	P_{app} AP (cm/sec × 10^{-5})[b]	P_{app} BL (cm/sec × 10^{-5})[c]	ER[d]
14	36 ± 2.2 μM	1.24 ± 0.113	1.65 ± 0.772	1.33
9d	43 ± 1.2 μM	1.98 ± 0.191	2.15 ± 0.322	1.09
15	>100 μM	0.496 ± 0.610	1.57 ± 0.574	3.17
12a	>100 μM	0.992 ± 0.984	1.49 ± 0.290	1.50
diazepam	n.d.	1.49 ± 0.323	1.37 ± 0.781	0.92
FD4	n.d.	0.874 ± 0.640	1.03 ± 0.210	1.18

[a] Cytotoxicity of compounds tested at concentrations in the range 0.1–100 μM in human neuroblastoma SH-SY5Y cell lines for 24 h. Data are reported as IC_{50} values, relative to untreated cells (control). Data represent means ± SD (n = 3).

[b] P_{app} AP is the apparent permeability of apical-to-basal transport expressed in cm/sec × 10^{-5}.

[c] P_{app} BL is the apparent permeability of basal-to-apical transport expressed in cm/sec × 10^{-5}.

[d] Efflux ratio (ER) was calculated using the following equation: $ER = P_{app}$ BL/P_{app} AP.

nusco sul Naviglio, Italy). Full-scan mass spectra were recorded in the mass/charge (*m*/*z*) range 50–3000 Da. Melting points for solid final compounds were determined by the capillary method on a Stuart Scientific SMP3 electrothermal apparatus and are uncorrected. The following intermediates have been already described in the literature: *tert*-butyl 4-{[(3,4-dimethyl-2-oxo-2*H*-chromen-7-yl)oxy]methyl}piperidine-1-carboxylate (**7a**) [28], 3,4-dimethyl-7-(piperidin-4-ylmethoxy)-2*H*-chromen-2-one (**8a**) [28], *tert*-butyl 3-{[(3,4-dimethyl-2-oxo-2*H*-chromen-7-yl)oxy]methyl}piperidine-1-carboxylate (**7f**) [28], 3,4-dimethyl-7-(piperidin-3-ylmethoxy)-2*H*-chromen-2-one (**8f**) [28], 7-hydroxy-4-methyl-coumarin [50], 7-hydroxy-3-methyl-coumarin [51], 7-hydroxy-3,4-dimethyl-coumarin (**4b**) [52], *tert*-butyl 4-{[(methylsulfonyl)oxy]methyl}piperidine-1-carboxylate [28], *tert*-butyl 3-{[(methylsulfonyl)oxy]methyl}piperidine-1-carboxylate [28].

*6.1.1. 4-(Chloromethyl)-7-{[4-(hydroxymethyl)benzyl]oxy}-2H-chromen-2-one **(2a)***

4-Chloromethyl-7-hydroxycoumarin [53] (0.21 g, 1.0 mmol) was suspended in dry acetonitrile (8 mL) before adding [4-(chloromethyl)-phenyl]methanol (0.78 g, 5.0 mmol) and potassium carbonate (0.14 g, 1.0 mmol). The reaction mixture was refluxed for 8 h and then the solid residue was filtered off. The solution was concentrated under rotary evaporation and purified through column chromatography (gradient eluent: methanol in dichloromethane 0%→5%). Pale yellow solid; yield: 0.26 g, 80%. ^{1}H NMR (500 MHz, Acetone-d_6) *δ*: 4.65 (s, 2H), 4.93 (s, 2H), 5.27 (s, 2H), 6.45 (s, 1H), 7.02 (d, *J* = 2.4 Hz, 1H),

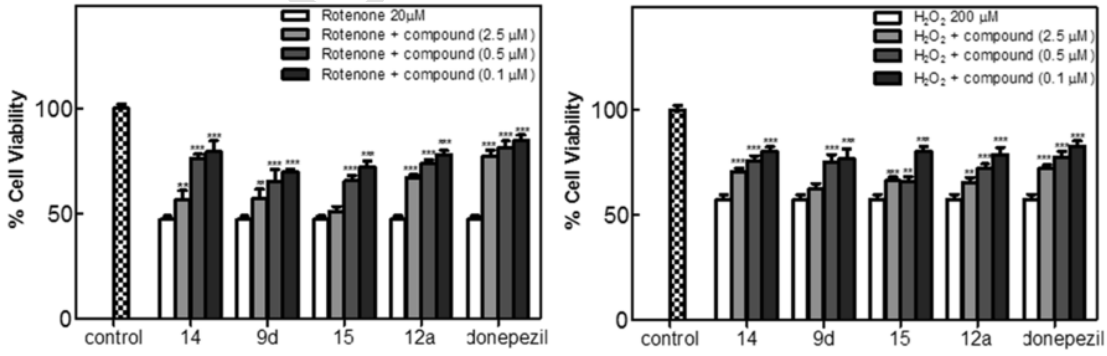

Fig. 8. Neuroprotective action on human neuroblastoma SH-SY5Y cells of nitrates **14**–**15** and alcohols **9d** and **12a** with rotenone (20 μM) or H_2O_2 (200 μM) after incubation at different concentrations (2.5, 0.5 or 0.1 μM). Cell proliferation was assessed by MTT assay. Data are expressed as percentage of viable cells (referred to untreated cells as control) and shown as mean ± SD (n = 3). Donepezil was used as a reference anti-AD marketed drug. Statistical significance was calculated using a two-way analysis of variance (ANOVA) followed by the Bonferroni post hoc tests (GraphPad Prism vers. 5); **p < 0.01, ***p < 0.001.

7.06 (dd, *J*=8.8, 2.4 Hz, 1H), 7.41 (d, *J*=8.3 Hz, 2H), 7.48 (d, *J*=8.3 Hz, 2H), 7.79 (d, *J*=8.8 Hz, 1H), OH not detected.

6.1.2. 4-[(Dimethylamino)methyl]-7-{[4-(hydroxymethyl)benzyl]oxy}-2H-chromen-2-one ***(3a)***

Intermediate **2a** (0.20 g, 0.60 mmol) was dissolved in dry THF (4 mL) and commercially available 2.0 N solution of *N*,*N*-dimethylamine in THF (0.90 mL, 1.8 mmol) was added. After stirring at room temperature for 6 h, the solvent and excess amine were evaporated under reduced pressure and the crude residue was purified through column chromatography (gradient eluent: methanol in dichloromethane 0%→5%). Pale yellow solid; yield: 0.18 g, 87%; mp: 93-5 °C. ^{1}H NMR (500 MHz, Acetone-d_6) δ: 2.29 (s, 6H, N(CH_3)$_2$), 3.58 (s, 2H, CH_2N), 4.65 (s, 2H, CH_2OH), 5.25 (s, 2H, CH_2OAr), 6.25 (s, 1H, 3-H$_{coum}$), 6.95 (d, *J*=2.5 Hz, 1H, 8-H$_{coum}$), 6.97 (dd, *J*=8.8, 2.5 Hz, 1H, 6-H$_{coum}$), 7.40 (d, *J*=8.3 Hz, 2H, H$_{Ar}$), 7.47 (d, *J*=8.3 Hz, 2H, H$_{Ar}$), 7.90 (d, *J*=8.8 Hz, 1H, 5-H$_{coum}$), OH not detected. Anal. ($C_{20}H_{21}NO_4$) calcd. % C, 70.78; H, 6.24; N, 4.13. Found % C, 70.82; H, 6.31; N, 4.04. HRMS (Q-TOF) calcd. for $C_{20}H_{21}NO_4$ [*M*+H]$^+$ *m/z* 340.1543, found 340.1541; [*M*+Na]$^+$ *m/z* 362.1363, found 362.1360.

6.1.3. 4-[(Dimethylamino)methyl]-7-{[3-(hydroxymethyl)benzyl]oxy}-2H-chromen-2-one ***(3b)***

[3-(Chloromethyl)-phenyl]methanol [54] (0.23 g, 1.5 mmol) and potassium carbonate (0.12 g, 0.90 mmol) were added to a stirred suspension of 4-[(dimethylamino)methyl]-7-hydroxy-2*H*-chromen-2-one (**2b**) [55] (0.13 g, 0.60 mmol) in dry acetonitrile (5 mL). After refluxing for 1 h, the residue was filtered and washed with dichloromethane. The solution was concentrated to dryness and purified through column chromatography (gradient eluent: methanol in dichloromethane 0%→5%). Colorless oil; yield: 0.15 g, 76%. ^{1}H NMR (500 MHz, DMSO-d_6) δ: 2.21 (s, 6H, N(CH_3)$_2$), 3.53 (s, 2H, CH_2N), 4.49 (d, *J*=5.4 Hz, 2H, CH_2OH), 5.19–5.21 (m, 3H, 1H dis. with D_2O, CH_2OAr + OH), 6.25 (s, 1H, 3-H$_{coum}$), 6.99 (dd, *J*=8.8, 2.5 Hz, 1H, 6-H$_{coum}$), 7.05 (d, *J*=2.5 Hz, 1H, 8-H$_{coum}$), 7.26–7.33 (m, 3H, 4-H$_{Ar}$ + 5-H$_{Ar}$ + 6-H$_{Ar}$), 7.41 (s, 1H, 2-H$_{Ar}$), 7.84 (d, *J*=8.8 Hz, 1H, 5-H$_{coum}$). Anal. ($C_{20}H_{21}NO_4$) calcd. % C, 70.78; H, 6.24; N, 4.13. Found % C, 70.94; H, 6.31; N, 3.99. HRMS (Q-TOF) calcd. for $C_{20}H_{21}NO_4$ [*M*+H]$^+$ *m/z* 340.1543, found 340.1540; [*M*+Na]$^+$ *m/z* 362.1363, found 362.1363.

6.1.4. 7-{[3-(Chloromethyl)benzyl]oxy}-4-(hydroxymethyl)-2H-chromen-2-one ***(5b)***

7-Hydroxy-4-(hydroxymethyl)-2*H*-chromen-2-one [56] (**4a**, 0.38 g, 2.0 mmol) was refluxed in dry acetonitrile (15 mL) in the presence of potassium carbonate (0.41 g, 3.0 mmol) and α,α′-dichloro-*m*-xylene (1.8 g, 10 mmol) for 5 h. After cooling to room temperature, the mixture was filtered and the solid was thoroughly washed with chloroform. The solution was concentrated to dryness and the crude residue was washed several times with *n*-hexane/diethyl ether 2/1 v/v mixture until removal of excess starting halide, thus yielding the desired **5b**. Off-white solid; yield: 0.58 g, 88%. ^{1}H NMR (300 MHz, DMSO-d_6) δ: 4.71 (s, 2H), 4.77 (s, 2H), 5.22 (s, 2H), 5.60 (s, 1H, dis. with D_2O), 6.28 (s, 1H), 6.99 (dd, *J*=8.8, 2.4 Hz, 1H), 7.08 (d, *J*=2.4 Hz, 1H), 7.33–7.46 (m, 3H), 7.54 (s, 1H), 7.61 (d, *J*=8.8 Hz, 1H).

6.1.5. 7-{[3-(Chloromethyl)benzyl]oxy}-3,4-dimethyl-2H-chromen-2-one ***(5c)***

7-Hydroxy-3,4-dimethyl-2*H*-chromen-2-one [28] (**4b**, 0.38 g, 2.0 mmol) was refluxed in dry acetonitrile (15 mL) in the presence of potassium carbonate (0.41 g, 3.0 mmol) and α,α′-dichloro-*m*-xylene (1.8 g, 10 mmol) for 8 h. After cooling to room temperature, the solvent was removed under rotary evaporation and the residue was purified through column chromatography (gradient eluent: ethyl acetate in *n*-hexane 10%→30%). White solid; yield: 0.43 g, 65%. ^{1}H NMR (500 MHz, DMSO-d_6) δ: 2.06 (s, 3H), 2.35 (s, 3H), 4.77 (s, 2H), 5.21 (s, 2H), 7.01 (dd, *J*=8.8, 2.4 Hz, 1H), 7.04 (d, *J*=2.4 Hz, 1H), 7.39–7.45 (m, 3H), 7.53 (s, 1H), 7.70 (d, *J*=8.8 Hz, 1H).

6.1.6. General procedure for the synthesis of 7-({4-[(dimethylamino)methyl]benzyl}oxy)-4-(hydroxymethyl)-2H-chromen-2-one ***(6a)*** *and 7-({3-[(dimethylamino)methyl]benzyl}oxy)-4-(hydroxymethyl)-2H-chromen-2-one* ***(6b)***

The appropriate intermediate 4-(hydroxymethyl)-7-(4-(bromomethyl)benzyloxy)coumarin (**5a**) [28] or **5b** (0.50 mmol) was dissolved in dry THF (4 mL) and 2.0 N solution of *N*,*N*-dimethylamine in THF (0.75 mL, 1.5 mmol) was added dropwise. After stirring at room temperature for 6 h, the reaction mixture was concentrated under vacuum and purified through column chromatography (gradient eluent: methanol in dichloromethane 0%→10%).

6.1.6.1. 7-({4-[(Dimethylamino)methyl]benzyl}oxy)-4-(hydroxymethyl)-2H-chromen-2-one ***(6a)***

Prepared from **5a** (0.19 g, 0.50 mmol) and 2.0 N solution of *N*,*N*-dimethylamine in THF (0.75 mL, 1.5 mmol). Pale yellow oil; yield: 0.15 g, 91%. ^{1}H NMR (500 MHz, DMSO-d_6) δ: 2.36 (s, 6H, N(CH_3)$_2$), 3.80 (s, 2H, CH_2N), 4.70 (d, *J*=5.4 Hz, 2H, CH_2OH), 5.21 (s, 2H, CH_2OAr), 5.60 (t, *J*=5.4 Hz, 1H, dis. with D_2O, OH), 6.28 (s, 1H, 3-H$_{coum}$), 6.99 (dd, *J*=8.8, 2.4 Hz, 1H, 6-H$_{coum}$), 7.07 (d, *J*=2.4 Hz, 1H, 8-H$_{coum}$), 7.38 (d, *J*=7.8 Hz, 2H, H$_{Ar}$), 7.46 (d, *J*=7.8 Hz, 2H, H$_{Ar}$), 7.60 (d, *J*=8.8 Hz, 1H, 5-H$_{coum}$). Anal. ($C_{20}H_{21}NO_4$) calcd. % C, 70.78; H, 6.24; N, 4.13. Found % C, 70.91; H, 6.36; N, 4.07. HRMS (Q-TOF) calcd. for $C_{20}H_{21}NO_4$ [*M*+H]$^+$ *m/z* 340.1543, found 340.1542; [*M*+Na]$^+$ *m/z* 362.1363, found 362.1365.

6.1.6.2. 7-({3-[(Dimethylamino)methyl]benzyl}oxy)-4-(hydroxymethyl)-2H-chromen-2-one ***(6b)***

Prepared from **5b** (0.17 g, 0.50 mmol) and 2.0 N solution of *N*,*N*-dimethylamine in THF (0.75 mL, 1.5 mmol). Colorless oil; yield: 0.095 g, 56%. ^{1}H NMR (500 MHz, DMSO-d_6) δ: 2.12 (s, 6H, N(CH_3)$_2$), 3.37 (s, 2H, CH_2N), 4.70 (d, *J*=5.4 Hz, 2H, CH_2OH), 5.19 (s, 2H, CH_2OAr), 5.60 (t, *J*=5.4 Hz, 1H, dis. with D_2O, OH), 6.28 (s, 1H, 3-H$_{coum}$), 6.99 (dd, *J*=8.8, 2.5 Hz, 1H, 6-H$_{coum}$), 7.06 (d, *J*=2.5 Hz, 1H, 8-H$_{coum}$), 7.22–7.24 (m, 1H, H$_{Ar}$), 7.32–7.33 (m, 2H, H$_{Ar}$), 7.37 (s, 1H, 2-H$_{Ar}$), 7.59 (d, *J*=8.8 Hz, 1H, 5-H$_{coum}$). Anal. ($C_{20}H_{21}NO_4$) calcd. % C, 70.78; H, 6.24; N, 4.13. Found % C, 70.86; H, 6.31; N, 4.08. HRMS (Q-TOF) calcd. for $C_{20}H_{21}NO_4$ [*M*+H]$^+$ *m/z* 340.1543, found 340.1541; [*M*+Na]$^+$ *m/z* 362.1363, found 362.1360.

6.1.7. 7-[(3-{[4-(Hydroxymethyl)piperidin-1-yl]methyl}benzyl)oxy]-3,4-dimethyl-2H-chromen-2-one ***(6c)***

Compound **5c** (0.16 g, 0.50 mmol) was dissolved in dry acetone (4 mL) and stirred with 4-piperidinemethanol (0.069 g, 0.60 mmol) in the presence of DIEA (0.13 mL, 0.75 mmol) at room temperature overnight. The solvent was removed under rotary evaporation and the crude oil was purified through column chromatography (gradient eluent: methanol in dichloromethane 0%→10%). Dark yellow oil; yield: 0.14 g, 67%. ^{1}H NMR (300 MHz, $CDCl_3$) δ: 1.54–1.68 (m, 3H, 3-H$_{a(piper)}$ + 4-H$_{(piper)}$), 1.76–1.91 (m, 2H, 3-H$_{b(piper)}$), 2.16 (s, 3H, 3-CH_3), 2.35 (s, 3H, 4-CH_3), 2.38–2.48 (m, 2H, 2-H$_{a(piper)}$), 3.15–3.33 (m, 2H, 2-H$_{b(piper)}$), 3.49 (d, *J*=4.2 Hz, 2H, CH_2OH), 3.92 (s, 2H, ArCH_2N), 5.12 (s, 2H, ArCH_2OCoum), 6.81 (d, *J*=2.4 Hz, 1H, 8-H$_{coum}$), 6.91 (dd, *J*=8.9, 2.4 Hz, 1H, 6-H$_{coum}$), 7.32–7.44 (m, 3H, 4-H$_{Ar}$ + 5-H$_{Ar}$ + 6-H$_{Ar}$), 7.47–7.51 (m, 2H, 2-H$_{Ar}$ + 5-H$_{coum}$), OH not detected. Anal. ($C_{25}H_{29}NO_4$) calcd. % C, 73.68; H, 7.17; N, 3.44. Found % C, 73.85; H, 7.28; N, 3.31. HRMS (Q-TOF) calcd. for

$C_{25}H_{29}NO_4$ $[M+H]^+$ *m/z* 408.2169, found 408.2166; $[M+Na]^+$ *m/z* 430.1989, found 430.1987.

6.1.8. General procedure for the synthesis of substituted tert-butyl 4-{[(2-oxo-2H-chromen-7-yl)oxy]alkyl}piperidine-1-carboxylate ***(7b-e)*** *and tert-outyl 3-{[(2-oxo-2H-chromen-7-yl)oxy]methyl}piperidine-1-carboxylate* ***(7g)***

By following a previously reported method [28], a mixture of the appropriate 7-hydroxycoumarin (7.0 mmol), the suitable mesylate ester (6.7 mmol), triethylamine (2.8 mL, 20 mmol) and cesium carbonate (2.3 g, 7.0 mmol) were heated in dry DMF (15 mL) at 70 °C for 72 h. Then the mixture was poured onto crushed ice. The filtrate was collected and washed with abundant water yielding the desired Boc-protected intermediates **7b-e**, **7g** that were deprotected without further purification.

6.1.8.1. tert-Butyl 4-{[(4-methyl-2-oxo-2H-chromen-7-yl)oxy]methyl}piperidine-1-carboxylate ***(7b)***

Prepared from 7-hydroxy-4-methyl-coumarin (1.2 g, 7.0 mmol) and *tert*-butyl 4-{[(methylsulfonyl)oxy]methyl}piperidine-1-carboxylate (2.0 g, 6.7 mmol). White solid; yield: 2.3 g, 93%. ^{1}H NMR (300 MHz, $CDCl_3$) *δ*: 1.22–1.37 (m, 2H), 1.46 (s, 9H), 1.63–1.85 (m, 3H), 2.39 (s, 3H), 2.62–2.78 (m, 2H), 3.85–3.87 (m, 2H), 4.10–4.18 (m, 2H), 6.13 (s, 1H), 6.79 (d, *J* = 2.5 Hz, 1H), 6.84 (dd, *J* = 8.8, 2.5 Hz, 1H), 7.48 (d, *J* = 8.8 Hz, 1H).

6.1.8.2. tert-Butyl 4-{[(3-methyl-2-oxo-2H-chromen-7-yl)oxy]methyl}piperidine-1-carboxylate ***(7c)***

Prepared from 7-hydroxy-3-methyl-coumarin (1.2 g, 7.0 mmol) and *tert*-butyl 4-{[(methylsulfonyl)oxy]methyl}piperidine-1-carboxylate (2.0 g, 6.7 mmol). White solid; yield: 2.2 g, 86%. ^{1}H NMR (300 MHz, DMSO-d_6) *δ*: 1.24–1.31 (m, 2H), 1.60 (s, 9H), 1.70–1.83 (m, 3H), 2.03 (s, 3H), 2.64–2.81 (m, 2H), 3.90–3.95 (m, 4H), 6.86–6.97 (m, 2H), 7.50 (d, *J* = 8.2 Hz, 1H), 7.79 (s, 1H).

6.1.8.3. tert-Butyl 4-{[(2-oxo-2H-chromen-7-yl)oxy]methyl}piperidine-1-carboxylate ***(7d)***

Prepared from commercially available 7-hydroxy-coumarin (1.1 g, 7.0 mmol) and *tert*-butyl 4-{[(methylsulfonyl)oxy]methyl}piperidine-1-carboxylate (2.0 g, 6.7 mmol). Pale yellow solid; yield: 2.2 g, 91%. ^{1}H NMR (500 MHz, Acetone-d_6) *δ*: 1.23–1.31 (m, 3H), 1.44 (s, 9H), 1.82–1.85 (m, 2H), 2.81–2.92 (m, 2H), 4.01 (d, *J* = 6.4 Hz, 2H), 4.12–4.18 (m, 2H), 6.21 (d, *J* = 9.3 Hz, 1H), 6.89 (d, *J* = 2.4 Hz, 1H), 6.94 (dd, *J* = 8.8, 2.4 Hz, 1H), 7.58 (d, *J* = 8.8 Hz, 1H), 7.90 (d, *J* = 9.3 Hz, 1H).

6.1.8.4. tert-Butyl 4-{2-[(methylsulfonyl)oxy]ethyl}piperidine-1-carboxylate

Commercially available *N*-Boc-4-piperidineethanol (2.3 g, 10 mmol) was dissolved in CH_2Cl_2 (30 mL) before the addition of triethylamine (5.7 mL, 40 mmol). The mixture was cooled to 0 °C with an external ice bath, and methanesulfonyl chloride (0.9 mL, 11 mmol) was added dropwise. After warming at room temperature, the reaction was kept under magnetic stirring for 3 h. The mixture was diluted with CH_2Cl_2 (70 mL) and washed with satd. aq. Na_2CO_3 (3 × 80 mL). The organic phase was dried over Na_2SO_4 and the evaporation of the solvent under reduced pressure yielded the desired product that was used without further purification. Pale yellow solid; yield: 2.4 g, 77%. ^{1}H NMR (500 MHz, DMSO-d_6) *δ*: 0.91–1.02 (m, 2H), 1.36 (s, 9H), 1.58–1.63 (m, 5H), 2.60–2.66 (m, 2H), 3.14 (s, 3H), 3.86–3.90 (m, 2H), 4.21 (t, *J* = 6.4 Hz, 2H).

6.1.8.5. tert-Butyl 4-{2-[(3,4-dimethyl-2-oxo-2H-chromen-7-yl)oxy]ethyl}piperidine-1-carboxylate ***(7e)***

Prepared from 7-hydroxy-3,4-dimethyl-coumarin (1.3 g, 7.0 mmol) and *tert*-butyl 4-{2-[(methylsulfonyl)oxy]ethyl}piperidine-1-carboxylate (2.0 g, 6.7 mmol). Off-white solid; yield: 2.1 g, 77%. ^{1}H NMR (300 MHz, DMSO-d_6) *δ*: 1.01–1.11 (m, 2H), 1.37 (s, 9H), 1.64–1.71 (m, 5H), 2.05 (s, 3H), 2.34 (s, 3H), 2.68–2.71 (m, 2H), 3.87–3.93 (m, 2H), 4.09 (t, *J* = 5.9 Hz, 2H), 6.89–6.93 (m, 2H), 7.67 (d, *J* = 8.8 Hz, 1H).

6.1.8.6. tert-Butyl 3-{[(2-oxo-2H-chromen-7-yl)oxy]methyl}piperidine-1-carboxylate ***(7g)***

Prepared from 7-hydroxy-coumarin (1.1 g, 7.0 mmol) and *tert*-butyl 3-{[(methylsulfonyl)oxy]methyl}piperidine-1-carboxylate (2.0 g, 6.7 mmol). White solid; yield: 2.0 g, 81%. ^{1}H NMR (500 MHz, Acetone-d_6) *δ*: 1.41–1.49 (m, 11H), 1.68–1.72 (m, 1H), 1.92–1.95 (m, 1H), 2.00–2.03 (m, 1H), 2.67–2.72 (m, 1H), 2.92–2.97 (m, 1H), 3.80–3.91 (m, 2H), 4.01–4.08 (m, 2H), 6.21 (d, *J* = 9.3 Hz, 1H), 6.91 (d, *J* = 2.4 Hz, 1H), 6.95 (dd, *J* = 8.8, 2.4 Hz, 1H), 7.58 (d, *J* = 8.8 Hz, 1H), 7.90 (d, *J* = 9.3 Hz, 1H).

6.1.9. General procedure for the synthesis of substituted 7-(piperidin-4-ylalkoxy)-2H-chromen-2-ones ***(8b-e)*** *and 7-(piperidin-3-ylmethoxy)-2H-chromen-2-one* ***(8g)***

The suitable coumarin **7b-e**, **7g** (5.0 mmol) was dissolved in dry CH_2Cl_2 (10 mL) followed by the dropwise addition of trifluoroacetic acid (3.0 mL) at 0 °C through an external ice bath. The reaction mixture was stirred at room temperature overnight and the solvents were removed under rotary evaporation. The crude oil residue was diluted with dichloromethane (50 mL) and washed with Na_2CO_3 (3 × 20 mL). The organic phase was dried over Na_2SO_4 and concentrated to dryness, thus obtaining a solid residue that was purified through column chromatography (5% methanol in dichloromethane) giving the desired coumarin **8b-e**, **8g** as solids.

6.1.9.1. 4-Methyl-7-(piperidin-4-ylmethoxy)-2H-chromen-2-one ***(8b)***

Prepared from **7b** (1.9 g, 5.0 mmol). Off-white solid; yield: 1.2 g, 91%. ^{1}H NMR (300 MHz,$CDCl_3$) *δ*: 1.40–1.51 (m, 2H), 1.82–1.96 (m, 3H), 2.05–2.12 (m, 2H), 2.40 (s, 3H), 2.90–2.98 (m, 2H), 3.89–3.94 (m, 2H), 6.13 (s, 1H), 6.79–6.86 (m, 2H), 7.50 (d, *J* = 8.8 Hz, 1H), NH not detected.

6.1.9.2. 3-Methyl-7-(piperidin-4-ylmethoxy)-2H-chromen-2-one ***(8c)***

Prepared from **7c** (1.9 g, 5.0 mmol). White solid; yield: 0.96 g, 70%. ^{1}H NMR (300 MHz, DMSO-d_6) *δ*: 1.21–1.28 (m, 2H), 1.71–1.77 (m, 2H), 1.89–1.93 (m, 1H), 2.04 (s, 3H), 2.59–2.64 (m, 2H), 3.06–3.09 (m, 2H), 3.90 (d, *J* = 6.4 Hz, 2H), 6.90 (dd, *J* = 8.8, 2.5 Hz, 1H), 6.95 (d, *J* = 2.5 Hz, 1H), 7.51 (d, *J* = 8.8 Hz, 1H), 7.79 (s, 1H), NH not detected.

6.1.9.3. 7-(Piperidin-4-ylmethoxy)-2H-chromen-2-one ***(8d)***

Prepared from **7d** (1.8 g, 5.0 mmol). Brown solid; yield: 1.1 g, 88%. ^{1}H NMR (500 MHz, DMSO-d_6) *δ*: 1.10–1.22 (m, 2H), 1.64–1.69 (m, 2H), 1.79–1.88 (m, 1H), 2.41–2.46 (m, 2H), 2.90–2.95 (m, 2H), 3.88 (d, *J* = 6.4 Hz, 2H), 6.26 (d, *J* = 9.3 Hz, 1H), 6.92 (dd, *J* = 8.8, 2.4 Hz, 1H), 6.96 (d, *J* = 2.4 Hz, 1H), 7.59 (d, *J* = 8.8 Hz, 1H), 7.97 (d, *J* = 9.3 Hz, 1H), NH not detected.

6.1.9.4. 3,4-Dimethyl-7-(2-piperidin-4-ylethoxy)-2H-chromen-2-one ***(8e)***

Prepared from **7e** (2.0 g, 5.0 mmol). White solid; yield: 1.1 g, 73%. ^{1}H NMR (500 MHz, DMSO-d_6) *δ*: 1.03–1.10 (m, 2H), 1.51–1.57 (m, 2H), 1.61–1.64 (m, 3H), 2.04 (s, 3H), 2.33 (s, 3H), 2.41–2.45 (m,

2H), 2.88–2.91 (m, 2H), 4.07 (t, *J*=6.4 Hz, 2H), 6.89–6.91 (m, 2H), 7.64 (d, *J*=8.8 Hz, 1H). NH not detected.

*6.1.9.5. 7-(Piperidin-3-ylmethoxy)-2H-chromen-2-one **(8g)***

Prepared from **7g** (1.8 g, 5.0 mmol). Pale yellow solid; yield: 1.3 g, 99%. ^{1}H NMR (500 MHz, DMSO-d_6) δ: 1.32–1.35 (m, 1H), 1.61–1.64 (m, 1H), 1.82–1.84 (m, 2H), 2.17–2.19 (m, 1H), 2.75–2.81 (m, 2H), 3.24–3.29 (m, 1H), 3.36–3.40 (m, 1H), 3.95–3.99 (m, 1H), 4.04–4.07 (m, 1H), 6.30 (d, *J*=9.3 Hz, 1H), 6.96 (dd, *J*=8.8, 2.4 Hz, 1H), 7.01 (d, *J*=2.4 Hz, 1H), 7.64 (d, *J*=8.8 Hz, 1H), 7.99 (d, *J*=9.3 Hz, 1H), NH not detected.

*6.1.10. General procedure for the synthesis of substituted 7-({1-[benzyl]piperidin-3-yl}methoxy)-2H-chromen-2-ones **(9a-b)** and 7-({1-[benzyl]piperidin-4-yl}methoxy)-2H-chromen-2-ones **(9c-h)***

The appropriate compound **8a-c** or **8f** (0.50 mmol) was suspended in dry acetonitrile (4 mL) followed by the addition of potassium carbonate (0.14 g, 1.0 mmol), 3- or [4-(chloromethyl)-phenyl]methanol [54] (0.094 g, 0.60 mmol) and a catalytic amount of potassium iodide. After refluxing for 6 h, the solvent was removed under rotary evaporation. The resulting crude was suspended in dichloromethane and the inorganic residue was filtered-off. The solution was concentrated to dryness and purified as indicated below to obtain final coumarins **9a-h** as white solids.

*6.1.10.1. 7-({1-[4-(Hydroxymethyl)benzyl]piperidin-3-yl}methoxy)-3,4-dimethyl-2H-chromen-2-one **(9a)***

[57] Prepared from **8f** (0.14 g, 0.50 mmol) and [4-(chloromethyl)-phenyl]methanol (0.094 g, 0.60 mmol). Purified through column chromatography (gradient eluent: methanol in dichloromethane from 0% to 5%). White solid; yield: 0.13 g, 64%; mp: 52-5 °C. ^{1}H NMR (300 MHz, Acetone-d_6) δ: 1.17–1.28 (m, 1H, 4-$H_{a(piper)}$), 1.50–1.61 (m, 1H, 5-$H_{a(piper)}$), 1.62–1.75 (m, 1H, 5-$H_{b(piper)}$), 1.80–1.87 (m, 1H, 4-$H_{b(piper)}$), 1.97–2.17 (m, 3H, 2-$H_{a(piper)}$ + 6-$H_{a(piper)}$ + 3-$H_{(piper)}$), 2.11 (s, 3H, 3-CH_3), 2.39 (s, 3H, 4-CH_3), 2.68–2.71 (m, 1H, 6-$H_{b(piper)}$), 2.83–2.94 (m, 1H, 2-$H_{b(piper)}$), 3.44 (d, *J*=13.4 Hz, 1H, ArCH_aN), 3.51 (d, *J*=13.4 Hz, 1H, ArCH_bN), 4.00 (d, *J*=6.4 Hz, 2H, CH_2OAr), 4.59 (s, 2H, CH_2OH), 6.82 (d, *J*=2.3 Hz, 1H, 8-H_{coum}), 6.88 (dd, *J*=8.8, 2.3 Hz, 1H, 6-H_{coum}), 7.27–7.30 (s, 4H, H_{Ar}), 7.65 (d, *J*=8.8 Hz, 1H, 5-H_{coum}), OH not detected. Anal. ($C_{25}H_{29}NO_4$) calcd. % C, 73.68; H, 7.17; N, 3.44. Found % C, 73.88; H, 7.21; N, 3.33. HRMS (Q-TOF) calcd. for $C_{25}H_{29}NO_4$ [*M*+H]$^+$ *m/z* 408.2169, found 408.2161; [*M*+Na]$^+$ *m/z* 430.1989, found 430.1991.

*6.1.10.2. 7-({1-[3-(Hydroxymethyl)benzyl]piperidin-3-yl}methoxy)-3,4-dimethyl-2H-chromen-2-one **(9b)***

[57] Prepared from **8f** (0.14 g, 0.50 mmol) and [3-(chloromethyl)-phenyl]methanol (0.094 g, 0.60 mmol). Purified through crystallization from hot ethanol 95%. White solid; yield: 0.18 g, 86%; mp: 118–120 °C. ^{1}H NMR (500 MHz, DMSO-d_6) δ: 1.07–1.14 (m, 1H, 4-$H_{a(piper)}$), 1.43–1.50 (m, 1H, 5-$H_{a(piper)}$), 1.60–1.64 (m, 1H, 5-$H_{b(piper)}$), 1.72–1.78 (m, 1H, 4-$H_{b(piper)}$), 1.86–2.03 (m, 3H, 2-$H_{a(piper)}$ + 6-$H_{a(piper)}$ + 3-$H_{(piper)}$), 2.05 (s, 3H, 3-CH_3), 2.34 (s, 3H, 4-CH_3), 2.62–2.66 (m, 1H, 6-$H_{b(piper)}$), 2.82–2.85 (m, 1H, 2-$H_{b(piper)}$), 3.40 (d, *J*=13.2 Hz, 1H, ArCH_aN), 3.43 (d, *J*=13.2 Hz, 1H, ArCH_bN), 3.92 (d, *J*=6.4 Hz, 2H, CH_2OAr), 4.44 (d, *J*=5.4 Hz, 2H, CH_2OH), 5.12 (t, *J*=5.4 Hz, 1H, dis. with D_2O, OH), 6.87–6.89 (m, 2H, 6-H_{coum} + 8-H_{coum}), 7.12 (d, *J*=7.5 Hz, 1H, H_{Ar}), 7.16 (d, *J*=7.5 Hz, 1H, H_{Ar}), 7.20–7.22 (m, 2H, H_{Ar}), 7.65 (d, *J*=8.8 Hz, 1H, 5-H_{coum}). Anal. ($C_{25}H_{29}NO_4$) calcd. % C, 73.68; H, 7.17; N, 3.44. Found % C, 73.75; H, 7.18; N, 3.39. HRMS (Q-TOF) calcd. for $C_{25}H_{29}NO_4$ [*M*+H]$^+$ *m/z* 408.2169, found 408.2169; [*M*+Na]$^+$ *m/z* 430.1989, found 430.1988.

*6.1.10.3. 7-({1-[4-(Hydroxymethyl)benzyl]piperidin-4-yl}methoxy)-3,4-dimethyl-2H-chromen-2-one **(9c)***

Prepared from **8a** (0.14 g, 0.50 mmol) and [4-(chloromethyl)-phenyl]methanol (0.094 g, 0.60 mmol). Purified through crystallization from hot ethanol 95%. White solid; yield: 0.13 g, 64%; mp: 157-9 °C. ^{1}H NMR (500 MHz, DMSO-d_6) δ: 1.24–1.33 (m, 2H, 3-$H_{a(piper)}$), 1.70–1.72 (m, 3H, 3-$H_{b(piper)}$ + 4-$H_{(piper)}$), 1.87–1.92 (m, 2H, 2-$H_{a(piper)}$), 2.04 (s, 3H, 3-CH_3), 2.33 (s, 3H, 4-CH_3), 2.78–2.82 (m, 2H, 2-$H_{b(piper)}$), 3.40 (s, 2H, ArCH_2N), 3.89 (d, *J*=5.9 Hz, 2H, CH_2OAr), 4.44 (d, *J*=5.9 Hz, 2H, CH_2OH), 5.11 (t, *J*=5.9 Hz, 1H, dis. with D_2O, OH), 6.90–6.93 (m, 2H, 6-H_{coum} + 8-H_{coum}), 7.21 (d, *J*=8.3 Hz, 2H, H_{Ar}), 7.23 (d, *J*=8.3 Hz, 2H, H_{Ar}), 7.65 (d, *J*=9.2 Hz, 1H, 5-H_{coum}). Anal. ($C_{25}H_{29}NO_4$) calcd. % C, 73.68; H, 7.17; N, 3.44. Found % C, 73.95; H, 7.28; N, 3.49. HRMS (Q-TOF) calcd. for $C_{25}H_{29}NO_4$ [*M*+H]$^+$ *m/z* 408.2169, found 408.2165; [*M*+Na]$^+$ *m/z* 430.1989, found 430.1990.

*6.1.10.4. 7-({1-[3-(Hydroxymethyl)benzyl]piperidin-4-yl}methoxy)-3,4-dimethyl-2H-chromen-2-one **(9d)***

Prepared from **8a** (0.14 g, 0.50 mmol) and [3-(chloromethyl)-phenyl]methanol (0.094 g, 0.60 mmol). Purified through column chromatography (gradient eluent: methanol in dichloromethane from 0% to 5%). White solid; yield: 0.16 g, 80%; mp: 128–130 °C. ^{1}H NMR (500 MHz, DMSO-d_6) δ: 1.26–1.33 (m, 2H, 3-$H_{a(piper)}$), 1.71–1.75 (m, 3H, 3-$H_{b(piper)}$ + 4-$H_{(piper)}$), 1.88–1.95 (m, 2H, 2-$H_{a(piper)}$), 2.05 (s, 3H, 3-CH_3), 2.34 (s, 3H, 4-CH_3), 2.80–2.83 (m, 2H, 2-$H_{b(piper)}$), 3.44 (s, 2H, ArCH_2N), 3.91 (d, *J*=6.4 Hz, 2H, CH_2OAr), 4.46 (d, *J*=5.4 Hz, 2H, CH_2OH), 5.13 (t, *J*=5.4 Hz, 1H, dis. with D_2O, OH), 6.90–6.93 (m, 2H, 6-H_{coum} + 8-H_{coum}), 7.12–7.16 (m, 2H, H_{Ar}), 7.22–7.27 (m, 2H, H_{Ar}), 7.66 (d, *J*=9.3 Hz, 1H, 5-H_{coum}). Anal. ($C_{25}H_{29}NO_4$) calcd. % C, 73.68; H, 7.17; N, 3.44. Found % C, 73.79; H, 7.18; N, 3.40. HRMS (Q-TOF) calcd. for $C_{25}H_{29}NO_4$ [*M*+H]$^+$ *m/z* 408.2169, found 408.2168; [*M*+Na]$^+$ *m/z* 430.1989, found 430.1988.

*6.1.10.5. 7-({1-[4-(Hydroxymethyl)benzyl]piperidin-4-yl}methoxy)-4-methyl-2H-chromen-2-one **(9e)***

Prepared from **8b** (0.14 g, 0.50 mmol) and [4-(chloromethyl)-phenyl]methanol (0.094 g, 0.60 mmol). Purified through column chromatography (gradient eluent: methanol in dichloromethane from 0% to 5%). White solid; yield: 0.10 g, 53%; mp: 103-5 °C. ^{1}H NMR (500 MHz, DMSO-d_6) δ: 1.26–1.33 (m, 2H, 3-$H_{a(piper)}$), 1.70–1.75 (m, 3H, 3-$H_{b(piper)}$ + 4-$H_{(piper)}$), 1.90–1.96 (m, 2H, 2-$H_{a(piper)}$), 2.37 (s, 3H, 4-CH_3), 2.79–2.83 (m, 2H, 2-$H_{b(piper)}$), 3.41 (s, 2H, ArCH_2N), 3.92 (d, *J*=7.5 Hz, 2H, CH_2OAr), 4.44 (d, *J*=5.8 Hz, 2H, CH_2OH), 5.09 (t, *J*=5.8 Hz, 1H, dis. with D_2O, OH), 6.18 (s, 1H, 3-H_{coum}), 6.92–6.96 (m, 2H, 6-H_{coum} + 8-H_{coum}), 7.22–7.26 (m, 4H, H_{Ar}), 7.65 (d, *J*=9.5 Hz, 1H, 5-H_{coum}). Anal. ($C_{24}H_{27}NO_4$) calcd. % C, 73.26; H, 6.92; N, 3.56. Found % C, 73.44; H, 6.99; N, 3.45. HRMS (Q-TOF) calcd. for $C_{24}H_{27}NO_4$ [*M*+H]$^+$ *m/z* 394.2013, found 394.2008; [*M*+Na]$^+$ *m/z* 416.1832, found 416.1831.

*6.1.10.6. 7-({1-[3-(Hydroxymethyl)benzyl]piperidin-4-yl}methoxy)-4-methyl-2H-chromen-2-one **(9f)***

Prepared from **8b** (0.14 g, 0.50 mmol) and [3-(chloromethyl)-phenyl]methanol (0.094 g, 0.60 mmol). Purified through column chromatography (gradient eluent: methanol in dichloromethane from 0% to 5%). White solid; yield: 0.12 g, 61%; mp: 146-8 °C. ^{1}H NMR (500 MHz, DMSO-d_6) δ: 1.26–1.33 (m, 2H, 3-$H_{a(piper)}$), 1.70–1.73 (m, 3H, 3-$H_{b(piper)}$ + 4-$H_{(piper)}$), 1.92–1.97 (m, 2H, 2-$H_{a(piper)}$), 2.37 (s, 3H, 4-CH_3), 2.80–2.83 (m, 2H, 2-$H_{b(piper)}$), 3.41 (s, 2H, ArCH_2N), 3.93 (d, *J*=5.8 Hz, 2H, CH_2OAr), 4.46 (d, *J*=5.8 Hz, 2H, CH_2OH), 5.12 (t, *J*=5.8 Hz, 1H, dis. with D_2O, OH), 6.18 (s, 1H, 3-H_{coum}), 6.93–6.95 (m, 2H, 6-H_{coum} + 8-H_{coum}), 7.12–7.17 (m, 2H, H_{Ar}), 7.21–7.26 (m,

2H, H_{Ar}), 7.65 (d, J=7.1 Hz, 1H, 5-H_{coum}). Anal. ($C_{24}H_{27}NO_4$) calcd. % C, 73.26; H, 6.92; N, 3.56. Found % C, 73.41; H, 7.00; N, 3.47. HRMS (Q-TOF) calcd. for $C_{24}H_{27}NO_4$ $[M+H]^+$ *m/z* 394.2013, found 394.2010; $[M+Na]^+$ *m/z* 416.1832, found 416.1831.

6.1.10.7. 7-({1-[4-(Hydroxymethyl)benzyl]piperidin-4-yl}methoxy)-3-methyl-2H-chromen-2-one hydrochloride ***(9g)***

Prepared from **8c** (0.14 g, 0.50 mmol) and [4-(chloromethyl)-phenyl]methanol (0.094 g, 0.60 mmol). Purified through column chromatography (gradient eluent: methanol in dichloromethane from 0% to 5%) and transformed into the hydrochloride salt with 4.0 N solution of HCl in dioxane. Off-white solid; yield: 0.095 g, 44%; mp: 163-4 °C. ^{1}H NMR (free base, 500 MHz, DMSO-d_6) δ: 1.24–1.32 (m, 2H, 3-$H_{a(piper)}$), 1.70–1.75 (m, 3H, 3-$H_{b(piper)}$ + 4-$H_{(piper)}$), 1.90–1.94 (m, 2H, 2-$H_{a(piper)}$), 2.03 (s, 3H, 3-CH_3), 2.79–2.81 (m, 2H, 2-$H_{b(piper)}$), 3.41 (s, 2H, ArCH_2N), 3.89 (d, J=6.5 Hz, 2H, CH_2OAr), 4.44 (d, J=6.2 Hz, 2H, CH_2OH), 5.09 (t, J=6.2 Hz, 1H, dis. with D_2O, OH), 6.91 (dd, J=8.8, 2.4 Hz, 1H, 6-H_{coum}), 6.94 (d, J=2.4 Hz, 1H, 8-H_{coum}), 7.20–7.26 (m, 4H, H_{Ar}), 7.49 (d, J=8.8 Hz, 1H, 5-H_{coum}), 7.78 (s, 1H, 4-H_{coum}). Anal. ($C_{24}H_{27}NO_4$·HCl) calcd. % C, 67.05; H, 6.56; N, 3.26. Found % C, 67.28; H, 6.68; N, 3.17. HRMS (Q-TOF) calcd. for $C_{24}H_{27}NO_4$ $[M+H]^+$ *m/z* 394.2013, found 394.2009; $[M+Na]^+$ *m/z* 416.1832, found 416.1829.

6.1.10.8. 7-({1-[3-(Hydroxymethyl)benzyl]piperidin-4-yl}methoxy)-3-methyl-2H-chromen-2-one hydrochloride ***(9h)***

Prepared from **8c** (0.14 g, 0.50 mmol) and [3-(chloromethyl)-phenyl]methanol (0.094 g, 0.60 mmol). Purified through column chromatography (gradient eluent: methanol in dichloromethane from 0% to 5%) and transformed into the hydrochloride salt with 4.0 N solution of HCl in dioxane. White solid; yield: 0.11 g, 50%; mp: 207-9 °C (dec.). ^{1}H NMR (300 MHz, DMSO-d_6) δ: 1.40–1.54 (m, 2H, 3-$H_{a(piper)}$), 1.77–2.01 (m, 3H, 3-$H_{b(piper)}$ + 4-$H_{(piper)}$), 2.03 (s, 3H, 3-CH_3), 2.89–3.01 (m, 2H, 2-$H_{a(piper)}$), 3.35–3.40 (m, 2H, 2-$H_{b(piper)}$), 3.91–3.94 (d, J=6.4 Hz, 2H, CH_2OAr), 4.27 (br d, 2H, ArCH_2NH^+), 4.51–4.54 (br d, 2H, CH_2OH), 5.29 (br s, 1H, dis. with D_2O, OH), 6.87–6.95 (m, 2H, 6-H_{coum} + 8-H_{coum}), 7.39–7.53 (m, 5H, H_{Ar} + 5-H_{coum}), 7.79 (s, 1H, 4-H_{coum}), 9.63 (s, 1H, dis. with D_2O, NH^+). Anal. ($C_{24}H_{27}NO_4$·HCl) calcd. % C, 67.05; H, 6.56; N, 3.26. Found % C, 67.35; H, 6.71; N, 3.08. HRMS (Q-TOF) calcd. for $C_{24}H_{27}NO_4$ $[M+H]^+$ *m/z* 394.2013, found 394.2011; $[M+Na]^+$ *m/z* 416.1832, found 416.1830.

6.1.11. 7-({1-[4-(2-Hydroxyethyl)benzyl]piperidin-4-yl}methoxy)-3,4-dimethyl-2H-chromen-2-one ***(9i)***

Intermediate **8a** (0.17 g, 0.60 mmol) was suspended in dry acetone (5 mL) and then DIEA (0.11 mL, 0.65 mmol) was added followed by 2-[4-(bromomethyl)phenyl]ethanol [27] (0.11 g, 0.50 mmol). After stirring overnight at room temperature, the mixture was concentrated to dryness and purified through column chromatography (gradient eluent: methanol in dichloromethane from 0% to 3%). Brown solid; yield: 0.099 g, 47%; mp: 86-8 °C (dec.). ^{1}H NMR (300 MHz, DMSO-d_6) δ: 1.13–1.33 (m, 2H, 3-$H_{a(piper)}$), 1.67–1.81 (m, 3H, 3-$H_{b(piper)}$ + 4-$H_{(piper)}$), 1.83–1.97 (m, 2H, 2-$H_{a(piper)}$), 2.05 (s, 3H, 3-CH_3), 2.34 (s, 3H, 4-CH_3), 2.59–2.75 (m, 2H, ArCH_2CH_2OH), 2.81–2.94 (m, 2H, 2-$H_{b(piper)}$), 3.38 (br s, 2H, ArCH_2N), 3.50–3.66 (m, 2H, CH_2OH), 3.93 (br s, 2H, CH_2OAr), 4.62 (br s, 1H, dis. with D_2O, OH), 6.86–6.99 (m, 2H, 6-H_{coum} + 8-H_{coum}), 7.05–7.47 (m, 4H, H_{Ar}), 7.67 (d, J=8.9 Hz, 1H, 5-H_{coum}). Anal. ($C_{26}H_{31}NO_4$) calcd. % C, 74.08; H, 7.41; N, 3.32. Found % C, 74.38; H, 7.59; N, 3.19. HRMS (Q-TOF) calcd. for $C_{26}H_{31}NO_4$ $[M+H]^+$ *m/z* 422.2326, found 422.2323; $[M+Na]^+$ *m/z* 444.2145, found 444.2142.

6.1.12. 7-{[1-(3-Hydroxybenzyl)piperidin-4-yl]methoxy}-3,4-dimethyl-2H-chromen-2-one ***(10)***

Coumarin **8a** (0.68 g, 2.4 mmol) was suspended in dry acetone (15 mL) followed by the addition of DIEA (0.42 mL, 2.4 mmol) and 3-chloromethylphenol [54] (0.28 g, 2.0 mmol). After stirring at room temperature for 7 h, the mixture was concentrated under rotary evaporation and purified through column chromatography (gradient eluent methanol in dichloromethane from 0% to 5%) furnishing the desired intermediate as an off-white solid. Yield: 0.52 g, 66%. ^{1}H NMR (300 MHz, DMSO-d_6) δ: 1.21–1.31 (m, 2H), 1.71–1.74 (m, 3H), 1.81–1.92 (m, 2H), 2.05 (s, 3H), 2.34 (s, 3H), 2.69–2.80 (m, 2H), 3.37 (s, 2H), 3.91 (d, J=5.3 Hz, 2H), 6.59–6.71 (m, 3H), 6.91–6.94 (m, 2H), 7.07 (t, J=7.0 Hz, 1H), 7.66 (d, J=9.9 Hz, 1H), 9.20 (s, 1H, dis. with D_2O).

6.1.13. 7-({1-[3-(3-Hydroxypropoxy)benzyl]piperidin-4-yl}methoxy)-3,4-dimethyl-2H-chromen-2-one ***(11)***

Phenol **10** (0.20 g, 0.50 mmol) was refluxed with potassium carbonate (0.14 g, 1.0 mmol), 3-bromopropan-1-ol (0.043 mL, 0.50 mmol) and a catalytic amount of KI in dry acetone (1.5 mL) for 8 h. The solvent was removed under vacuum and the resulting crude oil was purified through column chromatography (eluent: 5% methanol in dichloromethane) yielding a yellow solid. Yield: 0.12 g, 51%; mp: 74-6 °C. ^{1}H NMR (500 MHz, DMSO-d_6) δ: 1.25–1.33 (m, 2H, 3-$H_{a(piper)}$), 1.70–1.73 (m, 3H, 3-$H_{b(piper)}$ + 4-$H_{(piper)}$), 1.83 (qn, J=6.4 Hz, 2H, ArOCH_2CH_2CH_2OH), 1.88–1.96 (m, 2H, 2-$H_{a(piper)}$), 2.05 (s, 3H, 3-CH_3), 2.34 (s, 3H, 4-CH_3), 2.77–2.85 (m, 2H, 2-$H_{b(piper)}$), 3.40 (s, 2H, ArCH_2N), 3.53 (q, J=6.4 Hz, 2H, ArOCH_2CH_2CH_2OH), 3.91 (d, J=5.9 Hz, 2H, CH_2O-Coum), 3.98 (t, J=6.4 Hz, 2H, ArOCH_2CH_2CH_2OH), 4.50 (t, J=6.4 Hz, 1H, dis. with D_2O, OH), 6.76–6.79 (m, 1H, 4-H_{Ar}), 6.82–6.85 (m, 2H, 6-H_{Ar} + 2-H_{Ar}), 6.90–6.93 (m, 2H, 8-H_{coum} + 6-H_{coum}), 7.19 (t, J=7.3 Hz, 1H, 5-H_{Ar}), 7.67 (d, J=9.8 Hz, 1H, 5-H_{coum}). Anal. ($C_{27}H_{33}NO_5$) calcd. % C, 71.82; H, 7.37; N, 3.10. Found % C, 72.09; H, 7.50; N, 3.01. HRMS (Q-TOF) calcd. for $C_{27}H_{33}NO_5$ $[M+H]^+$ *m/z* 452.2431, found 452.2426; $[M+Na]^+$ *m/z* 474.2251, found 474.2252.

6.1.14. General procedure for the synthesis of substituted 7-{[1-(ω-hydroxyalkyl)piperidin-4-yl]methoxy}-2H-chromen-2-ones ***(12a-d)*** *and 7-{[1-(3-hydroxypropyl)piperidin-3-yl]methoxy}-2H-chromen-2-ones* ***(12e-f)***

The suitable unprotected piperidine **8a**, **8d-g** (0.50 mmol) was suspended in dry acetonitrile (5 mL). Potassium carbonate (0.10 g, 0.75 mmol), 3-bromo-1-propanol (0.090 mL, 1.0 mmol, for **12a-b** and **12d-f**) or 4-chlorobutan-1-ol (0.10 mL, 1.0 mmol, for **12c**), and a catalytic amount of KI were added and the mixture was refluxed for 4–6 h. The solvent was evaporated under reduced pressure and the solid residue was filtered-off after washing with CH_2Cl_2. The solution was concentrated to dryness, and the resulting crude product was purified as detailed below.

6.1.14.1. 7-{[1-(3-Hydroxypropyl)piperidin-4-yl]methoxy}-3,4-dimethyl-2H-chromen-2-one ***(12a)***

Prepared from **8a** (0.14 g, 0.50 mmol) and 3-bromo-1-propanol (0.090 mL, 1.0 mmol). Purified through crystallization from hot ethanol. White solid; yield: 0.12 g, 68%; mp: 117-9 °C. ^{1}H NMR (500 MHz, DMSO-d_6) δ: 1.22–1.29 (m, 2H, 3-$H_{a(piper)}$), 1.55 (qn, J=6.9 Hz, 2H, NCH_2CH_2CH_2OH), 1.71–1.76 (m, 3H, 3-$H_{b(piper)}$ + 4-$H_{(piper)}$), 1.80–1.86 (m, 2H, 2-$H_{a(piper)}$), 2.05 (s, 3H, 3-CH_3), 2.30 (t, J=6.9 Hz, 2H, NCH_2CH_2CH_2OH), 2.34 (s, 3H, 4-CH_3), 2.85–2.87 (m, 2H, 2-$H_{b(piper)}$), 3.41 (t, J=6.9 Hz, 2H, CH_2OH), 3.90 (d, J=5.9 Hz, 2H, CH_2OAr), 6.90–6.93 (m, 2H, 6-H_{coum} + 8-H_{coum}), 7.67 (d, J=8.8 Hz, 1H, 5-H_{coum}), OH not detected. Anal. ($C_{20}H_{27}NO_4$)

calcd. % C, 69.54; H, 7.88; N, 4.05. Found % C, 69.69; H, 7.96; N, 3.98. HRMS (Q-TOF) calcd. for $C_{20}H_{27}NO_4$ [*M*+H]$^+$ *m/z* 346.2013, found 346.2011; [*M*+Na]$^+$ *m/z* 368.1832, found 368.1830.

6.1.14.2. 7-{[1-(3-Hydroxypropyl)piperidin-4-yl]methoxy}-2H-chromen-2-one ***(12b)***

Prepared from **8d** (0.13 g, 0.50 mmol) and 3-bromo-1-propanol (0.090 mL, 1.0 mmol). Purified through column chromatography (gradient eluent: methanol in dichloromethane from 0% to 10%). White solid; yield: 0.063 g, 40%; mp: 137-9 °C (dec.). ^{1}H NMR (500 MHz, DMSO-d_6) δ: 1.27–1.34 (m, 2H, 3-H$_{a(piper)}$), 1.63 (qn, *J*=6.4 Hz, 2H, NCH$_2$C*H*$_2$CH$_2$OH), 1.78–1.85 (m, 3H, 3-H$_{b(piper)}$ + 4-H$_{(piper)}$), 2.13–2.27 (m, 2H, 2-H$_{a(piper)}$), 2.56 (br s, 2H, NC*H*$_2$CH$_2$CH$_2$OH), 2.92–3.06 (m, 2H, 2-H$_{b(piper)}$), 3.42 (t, *J*=6.4 Hz, 2H, C*H*$_2$OH), 3.93 (d, *J*=5.9 Hz, 2H, CH$_2$OAr), 6.26 (d, *J*=9.5 Hz, 1H, 3-H$_{coum}$), 6.93 (dd, *J*=8.6, 2.4 Hz, 1H, 6-H$_{coum}$), 6.94 (d, *J*=2.4 Hz, 1H, 8-H$_{coum}$), 7.60 (d, *J*=8.6 Hz, 1H, 5-H$_{coum}$), 7.97 (d, *J*=9.5 Hz, 1H, 4-H$_{coum}$), OH not detected. Anal. ($C_{18}H_{23}NO_4$) calcd. % C, 68.12; H, 7.30; N, 4.41. Found % C, 68.33; H, 7.33; N, 4.35. HRMS (Q-TOF) calcd. for $C_{18}H_{23}NO_4$ [*M*+H]$^+$ *m/z* 318.1700, found 318.1700; [*M*+Na]$^+$ *m/z* 340.1519, found 340.1515.

6.1.14.3. 7-((1-(4-Hydroxybutyl)piperidin-4-yl)methoxy)-3,4-dimethyl-2H-chromen-2-one ***(12c)***

Prepared from **8a** (0.14 g, 0.50 mmol) and 4-chloro-1-butanol (0.10 mL, 1.0 mmol). Purified through column chromatography (gradient eluent: methanol in dichloromethane from 0% to 10%). White solid; yield: 0.072 g, 40%; mp: 125-7 °C. ^{1}H NMR (300 MHz, DMSO-d_6) δ: 1.21–1.28 (m, 2H, 3-H$_{a(piper)}$), 1.38–1.46 (m, 4H, NCH$_2$C*H*$_2$C*H*$_2$CH$_2$OH), 1.70–1.78 (m, 3H, 3-H$_{b(piper)}$ + 4-H$_{(piper)}$), 1.80–1.92 (m, 2H, 2-H$_{a(piper)}$), 2.05 (s, 3H, 3-CH$_3$), 2.21–2.29 (m, 2H, NC*H*$_2$CH$_2$CH$_2$CH$_2$OH), 2.36 (s, 3H, 4-CH$_3$), 2.85–2.88 (m, 2H, 2-H$_{b(piper)}$), 3.36–3.39 (m, 2H, C*H*$_2$OH), 3.89–3.91 (m, 2H, CH$_2$OAr), 6.92–6.94 (m, 2H, 6-H$_{coum}$ + 8-H$_{coum}$), 7.66 (d, *J*=9.4 Hz, 1H, 5-H$_{coum}$), OH not detected. Anal. ($C_{21}H_{29}NO_4$) calcd. % C, 70.17; H, 8.13; N, 3.90. Found % C, 70.44; H, 8.22; N, 3.84. HRMS (Q-TOF) calcd. for $C_{21}H_{29}NO_4$ [*M*+H]$^+$ *m/z* 360.2169, found 360.2165; [*M*+Na]$^+$ *m/z* 382.1989, found 382.1991.

6.1.14.4. 7-{2-[1-(3-Hydroxypropyl)piperidin-4-yl]ethoxy}-3,4-dimethyl-2H-chromen-2-one ***(12d)***

Prepared from **8e** (0.15 g, 0.50 mmol) and 3-bromo-1-propanol (0.090 mL, 1.0 mmol). Purified through column chromatography (gradient eluent: methanol in dichloromethane from 0% to 10%). White solid; yield: 0.13 g, 71%; mp: 97-9 °C. ^{1}H NMR (500 MHz, DMSO-d_6) δ: 1.15–1.21 (m, 3H, 3-H$_{a(piper)}$ + 4-H$_{(piper)}$), 1.56 (qn, *J*=6.4 Hz, 2H, NCH$_2$C*H*$_2$CH$_2$OH), 1.63–1.70 (m, 4H, C*H*$_2$CH$_2$OAr + 3-H$_{b(piper)}$), 1.88–1.92 (m, 2H, 2-H$_{a(piper)}$), 2.05 (s, 3H, 3-CH$_3$), 2.34 (s, 3H, 4-CH$_3$), 2.32–2.36 (m, 2H, NC*H*$_2$CH$_2$CH$_2$OH), 2.88 (br s, 2H, 2-H$_{b(piper)}$), 3.41 (t, *J*=6.4 Hz, 2H, C*H*$_2$OH), 4.08 (t, *J*=6.9 Hz, 2H, CH$_2$C*H*$_2$OAr), 6.90–6.93 (m, 2H, 6-H$_{coum}$ + 8-H$_{coum}$), 7.66 (d, *J*=8.8 Hz, 1H, 5-H$_{coum}$), OH not detected. Anal. ($C_{21}H_{29}NO_4$) calcd. % C, 70.17; H, 8.13; N, 3.90. Found % C, 70.21; H, 8.05; N, 3.91. HRMS (Q-TOF) calcd. for $C_{21}H_{29}NO_4$ [*M*+H]$^+$ *m/z* 360.2169, found 360.2167; [*M*+Na]$^+$ *m/z* 382.1989, found 382.1984.

6.1.14.5. 7-{[1-(3-Hydroxypropyl)piperidin-3-yl]methoxy}-3,4-dimethyl-2H-chromen-2-one ***(12e)***

[57] Prepared from **8f** (0.14 g, 0.50 mmol) and 3-bromo-1-propanol (0.090 mL, 1.0 mmol). Purified through column chromatography (gradient eluent: methanol in dichloromethane from 0% to 10%). Off-white solid; yield: 0.093 g, 54%; mp 104-7 °C. ^{1}H NMR (500 MHz, DMSO-d_6) δ: 1.05–1.16 (m, 1H, 4-H$_{a(piper)}$), 1.39–1.53 (m, 1H, 5-H$_{a(piper)}$), 1.58 (qn, *J*=6.3 Hz, 2H, NCH$_2$C*H*$_2$CH$_2$OH), 1.62–1.69 (m, 1H, 5-H$_{b(piper)}$), 1.69–1.78 (m, 1H, 4-H$_{b(piper)}$), 1.85–1.95 (m, 1H, 2-H$_{a(piper)}$), 1.95–2.03 (m, 2H, 6-H$_{a(piper)}$ + 3-H$_{(piper)}$), 2.05 (s, 3H, 3-CH$_3$), 2.36 (s, 3H, 4-CH$_3$), 2.38 (br s, 2H, NC*H*$_2$CH$_2$CH$_2$OH), 2.73–2.81 (m, 1H, 6-H$_{b(piper)}$), 2.89–2.96 (m, 1H, 2-H$_{b(piper)}$), 3.41 (t, *J*=6.3 Hz, 2H, C*H*$_2$OH), 3.89–3.98 (m, 2H, CH$_2$OAr), 6.90–6.95 (m, 2H, 6-H$_{coum}$ + 8-H$_{coum}$), 7.66 (d, *J*=9.5 Hz, 1H, 5-H$_{coum}$), OH not detected. Anal. ($C_{20}H_{27}NO_4$) calcd. % C, 69.54; H, 7.88; N, 4.05. Found % C, 69.82; H, 7.95; N, 3.88. HRMS (Q-TOF) calcd. for $C_{20}H_{27}NO_4$ [*M*+H]$^+$ *m/z* 346.2013, found 346.2011; [*M*+Na]$^+$ *m/z* 368.1832, found 368.1834.

6.1.14.6. 7-{[1-(3-Hydroxypropyl)piperidin-3-yl]methoxy}-2H-chromen-2-one ***(12f)***

Prepared from **8g** (0.13 g, 0.50 mmol) and 3-bromo-1-propanol (0.090 mL, 1.0 mmol). Purified through crystallization from hot ethanol. Off-white solid; yield: 0.11 g, 69%; mp: 175-7 °C. ^{1}H NMR (500 MHz, DMSO-d_6) δ: 1.08–1.12 (m, 1H, 4-H$_{a(piper)}$), 1.45–1.49 (m, 1H, 5-H$_{a(piper)}$), 1.55–1.57 (m, 2H, NCH$_2$C*H*$_2$CH$_2$OH), 1.63–1.65 (m, 1H, 5-H$_{b(piper)}$), 1.71–1.73 (m, 1H, 4-H$_{b(piper)}$), 1.87–1.98 (m, 3H, 2-H$_{a(piper)}$ + 6-H$_{a(piper)}$ + 3-H$_{(piper)}$), 2.31–2.40 (m, 2H, NC*H*$_2$CH$_2$CH$_2$OH), 2.72–2.74 (m, 1H, 6-H$_{b(piper)}$), 2.89–2.91 (m, 1H, 2-H$_{b(piper)}$), 3.40 (t, *J*=6.4 Hz, 2H, C*H*$_2$OH), 3.93–3.95 (m, 2H, CH$_2$OAr), 6.26 (d, *J*=9.3 Hz, 1H, 3-H$_{coum}$), 6.93 (dd, *J*=8.8, 2.4 Hz, 1H, 6-H$_{coum}$), 6.96 (d, *J*=2.4 Hz, 1H, 8-H$_{coum}$), 7.60 (d, *J*=8.8 Hz, 1H, 5-H$_{coum}$), 7.96 (d, *J*=9.3 Hz, 1H, 4-H$_{coum}$), OH not detected. Anal. ($C_{18}H_{23}NO_4$) calcd. % C, 68.12; H, 7.30; N, 4.41. Found % C, 68.40; H, 7.36; N, 4.29. HRMS (Q-TOF) calcd. for $C_{18}H_{23}NO_4$ [*M*+H]$^+$ *m/z* 318.1700, found 318.1696; [*M*+Na]$^+$ *m/z* 340.1519, found 340.1518.

6.1.15. 7-({1-[3-(Chloromethyl)benzyl]piperidin-4-yl}methoxy)-3,4-dimethyl-2H-chromen-2-one ***(13)***

Coumarin **8a** (0.28 g, 1.0 mmol) was suspended in dry acetone (8 mL) before the addition of DIEA (0.17 mL, 1.0 mmol) and α,α′-dichloro-*m*-xylene (0.52 g, 3.0 mmol). The mixture was stirred at room temperature overnight and then the solvent was removed under vacuum. The resulting crude was purified through column chromatography (eluent: ethyl acetate in dichloromethane 50%). Yellow solid; yield: 0.31 g, 73%. ^{1}H NMR (300 MHz, $CDCl_3$) δ: 1.24–1.33 (m, 2H), 1.71–1.74 (m, 3H), 1.81–1.85 (m, 2H), 2.04 (s, 3H), 2.32 (s, 3H), 2.76–2.82 (m, 2H), 3.39 (s, 2H), 3.90–3.94 (m, 2H), 4.71 (s, 2H), 6.91–6.95 (m, 2H), 7.39–7.43 (m, 3H), 7.50 (s, 1H), 7.68 (d, *J*=8.8 Hz, 1H).

6.1.16. 3-[(4-{[(3,4-Dimethyl-2-oxo-2H-chromen-7-yl)oxy]methyl}piperidin-1-yl)methyl]benzyl nitrate ***(14)***

Intermediate **13** (0.26 g, 0.60 mmol) was refluxed in dry acetonitrile (4 mL) in the presence of $AgNO_3$ (0.30 g, 1.8 mmol) for 6 h. After cooling, the inorganic residue was filtered off. The solution was concentrated under rotary evaporation and purified through column chromatography (gradient eluent: methanol in dichloromethane from 0% to 5%) yielding the desired nitrate as a brown solid. Yield: 0.13 g, 48%. ^{1}H NMR (500 MHz, $CDCl_3$) δ: 1.43–1.60 (m, 2H, 3-H$_{a(piper)}$), 1.79–1.85 (m, 3H, 4-H$_{(piper)}$ + 3-H$_{b(piper)}$), 1.99–2.03 (m, 2H, 2-H$_{a(piper)}$), 2.18 (s, 3H, 3-CH$_3$), 2.36 (s, 3H, 4-CH$_3$), 2.91–2.97 (m, 2H, 2-H$_{b(piper)}$), 3.54 (br s, 2H, ArCH$_2$N), 3.92 (d, *J*=5.9 Hz, 2H, CH$_2$OAr), 5.47 (s, 2H, CH$_2$ONO$_2$), 6.73–6.81 (m, 2H, 6-H$_{coum}$ + 8-H$_{coum}$), 7.48–7.52 (m, 3H, 4-H$_{Ar}$ + 5-H$_{Ar}$ + 6-H$_{Ar}$), 7.70 (s, 1H, 2-H$_{Ar}$), 7.78 (d, *J*=8.8 Hz, 1H, 5-H$_{coum}$). Anal. ($C_{25}H_{28}N_2O_6$) calcd. % C, 66.36; H, 6.24; N, 6.19. Found % C, 66.45; H, 6.38; N, 6.03. HRMS (Q-TOF) calcd. for $C_{25}H_{28}N_2O_6$ [*M*+H]$^+$ *m/z* 453.2020, found 453.2023.

*6.1.17. General procedure for the synthesis of 3-(4-{[(3,4-dimethyl-2-oxo-2H-chromen-7-yl)oxy]methyl}piperidin-1-yl)propyl nitrate **(15)** and 3-{3-[(4-{[(3,4-dimethyl-2-oxo-2H-chromen-7-yl)oxy]methyl}piperidin-1-yl)methyl]phenoxy}propyl nitrate **(16)***

The appropriate piperidine **8a** or **10** (0.60 mmol) was suspended in dry acetonitrile (5 mL) before adding K_2CO_3 (0.13 g, 0.90 mmol) and 3-bromopropyl nitrate [39] (0.17 g, 0.90 mmol). The mixture was stirred at room temperature (24 h, for **15**) or refluxed (4 h, for **16**), and then concentrated to dryness. The resulting crude was treated with chloroform and filtered. The solution was then purified through column chromatography (gradient eluent: methanol in dichloromethane from 0% to 3%).

*6.1.17.1. 3-(4-{[(3,4-Dimethyl-2-oxo-2H-chromen-7-yl)oxy]methyl}piperidin-1-yl)propyl nitrate **(15)***

Prepared from **8a** (0.17 g, 0.60 mmol) and 3-bromopropyl nitrate (0.17 g, 0.90 mmol). Brown solid; yield: 0.12 g, 53%. ^{1}H NMR (500 MHz, $CDCl_3$) δ: 1.40–1.44 (m, 2H, 3-$H_{a(piper)}$), 1.81–1.84 (m, 3H, 4-$H_{(piper)}$ + 3-$H_{b(piper)}$), 1.95 (qn, J=6.4 Hz, 2H, $NCH_2CH_2CH_2ONO_2$), 2.00–2.05 (m, 2H, 2-$H_{a(piper)}$), 2.17 (s, 3H, 3-CH_3), 2.37 (s, 3H, 4-CH_3), 2.47 (t, J=6.4 Hz, 2H, $NCH_2CH_2CH_2ONO_2$), 2.95–2.99 (m, 2H, 2-$H_{b(piper)}$), 3.85 (d, J=5.9 Hz, 2H, CH_2OAr), 4.56 (t, J=6.4 Hz, 2H, CH_2ONO_2), 6.75 (d, J=2.4 Hz, 1H, 8-H_{coum}), 6.82 (dd, J=8.8, 2.4 Hz, 1H, 6-H_{coum}), 7.50 (d. J=8.8 Hz, 1H, 5-H_{coum}). Anal. ($C_{20}H_{26}N_2O_6$) calcd. % C, 61.53; H, 6.71; N, 7.18. Found % C, 61.64; H, 6.80; N, 7.05. HRMS (Q-TOF) calcd. for $C_{20}H_{26}N_2O_6$ $[M+H]^+$ *m/z* 391.1864, found 391.1865; $[M+Na]^+$ *m/z* 413.1683, found 413.1682.

*6.1.17.2. 3-{3-[(4-{[(3,4-Dimethyl-2-oxo-2H-chromen-7-yl)oxy]methyl}piperidin-1-yl)methyl]phenoxy}propyl nitrate **(16)***

Prepared from **10** (0.24 g, 0.60 mmol) and 3-bromopropyl nitrate (0.17 g, 0.90 mmol). Brown solid; yield: 0.11 g, 36%. ^{1}H NMR (500 MHz, $CDCl_3$) δ: 1.42–1.44 (m, 2H, 3-$H_{a(piper)}$), 1.79–1.82 (m, 3H, 3-$H_{b(piper)}$ + 4-$H_{(piper)}$), 1.98–2.02 (m, 2H, 2-$H_{a(piper)}$), 2.18 (s, 3H, 3-CH_3), 2.20–2.22 (m, 2H, $OCH_2CH_2CH_2ONO_2$), 2.36 (s, 3H, 4-CH_3), 2.91–2.94 (m, 2H, 2-$H_{b(piper)}$), 3.48 (s, 2H, $ArCH_2N$), 3.84–3.87 (m, 2H, CH_2OCoum), 4.07–4.09 (m, 2H, CH_2OAr), 4.67 (t, J=6.4 Hz, 2H, CH_2ONO_2), 6.77–6.83 (m, 3H, 6-H_{coum} + 8-H_{coum} + H_{Ar}), 6.89–6.92 (m, 2H, H_{Ar}), 7.20–7.24 (m, 1H, H_{Ar}), 7.47 (d, J=8.8 Hz, 1H, 5-H_{coum}). Anal. ($C_{27}H_{32}N_2O_7$) calcd. % C, 65.31; H, 6.50; N, 5.64. Found % C, 65.60; H, 6.56; N, 5.52. HRMS (Q-TOF) calcd. for $C_{27}H_{32}N_2O_7$ $[M+H]^+$ *m/z* 497.2282, found 497.2281.

6.2. In vitro inhibition assays

Inhibitory activities were determined through the protocols described as follows by means of nonlinear regressions of response/log(concentration) curve obtained with GraphPad Prism 5.0 software and are expressed as IC_{50} (μM) or as percentage of inhibition at 10 μM for less active compounds. Results are the mean of three independent experiments.

6.2.1. Fluoroscence-based MAOs inhibition assays

As already reported [27], human recombinant MAO A and MAO B (microsomes from baculovirus infected insect cells; Sigma-Aldrich) were used to determine IC_{50}s through a fluorescence-based method, using kynuramine as non-selective MAO A and MAO B substrate. Samples were pre-incubated 20 min at 37 °C before adding MAO solutions, then incubated for additional 30 min. Fluorescence was recorded at excitation/emission wavelengths of 310/400 nm (5 nm slit width for both excitation and emission) in a 96-well microplate fluorescence reader (Tecan Infinite M1000 Pro). Experiments were performed in triplicates in black, round-bottomed polystyrene 96-well microtiter plates (Greiner).

6.2.2. Direct kynuramine MAOs inhibition assay

Coumarins are well-known fluorescent molecules that may interfere with kynuramine-based MAOs inhibition assay protocol here applied. In order to rule out artifacts arising from samples fluorescent properties, an additional spectrophotometric in vitro protocol has been employed to test four compounds as hMAO B inhibitors bearing prototypes of different fluorescent moieties (**3a**: 4-[(dimethylamino)methyl]-7-hydroxy-2*H*-chromen-2-one; **6a**: 7-hydroxy-4-(hydroxymethyl)-2*H*-chromen-2-one; **9c**; 7-hydroxy-3,4-dimethyl-2*H*-chromen-2-one, **12b**; 7-hydroxy-2*H*-chromen-2-one). Data have been reported in Table S2 (Supporting Information) and are in agreement with the fluorescent method. In any case, this direct assay suffers from a low method sensitivity due to the product (4-hydroxyquinoline) absorbance at 316 nm, $\Delta\varepsilon = 12{,}000\ M^{-1}\,cm^{-1}$.

6.2.3. ChEs inhibition assay

Inhibition tests on ChEs were performed in vitro on AChE from electric eel (463 U/mg; Sigma) or human recombinant AChE (2770 U/mg; Sigma), BChE from equine serum (13 U/mg; Sigma) or BChE from human serum (50 U/mg; Sigma), by adapting the well-known spectrophotometric Ellman's method to a 96-well plate procedure [58]. Experiments were performed in triplicates in transparent, flat-bottomed polystyrene 96-well microtiter plates.

6.3. Griess assay

Aliquots (150 μL) from 1 mM stock solutions in DMSO of nitrate under study were added to DMSO (50 μL) and 800 μL of phosphate buffer (50 mM, pH = 7.40) containing 5 mM cysteine. Compounds were incubated in the dark at 37 °C. At appropriate time intervals ranging from 30 to 180 min, 250 μL of Griess reagent (4.0 g of sulphanilamide, 0.20 g of *N*-naphthylethylenediamine dihydrochloride, 10 mL of 85% phosphoric acid in distilled water to a final volume of 100 mL) were added. After 30 min in the dark at room temperature, absorbance was read at 540 nm using an Agilent 8453E UV-visible spectrophotometer equipped with a cell changer. NO release (quantitated as NO_2^-, μg/mL) was measured from the calibration curve derived from standard sodium nitrite solutions (0.005, 0.01, 0.02, 0.05, 0.07, 0.10, 0.20, and 0.40 μg/mL). Each compound was tested in triplicates.

6.4. Reversed-phase HPLC analysis

Following a protocol similar to studies already reported by us [59] to assess the hydrolytic stability in buffer and in the presence of thiols, 150 μL of 1 mM stock solutions of compounds **14**–**16** in DMSO were added to 1.350 mL of aqueous buffer solution (50 mM phosphate buffer, pH 7.40, 0.20 M KCl) or to 1.350 mL of buffer enriched with cysteine or glutathione (50 mM phosphate buffer, pH 7.40, 0.20 M KCl, 1 mM thiol) thus incubating final compounds concentration equal to 100 μM. Regarding serum stability experiments, a volume of 15 μL from 10 mM stock solutions of compounds **14**–**16** in DMSO was added to 1.485 mL of reconstituted human serum preheated at 37 ± 0.5 °C (final compound concentrations 100 μM).

For the analysis in cytosolic fractions, each sample was prepared from five dishes of SH-SY5Y cells, each containing 5.000.000 cells, that were collected and homogenized in 2 mL of Dulbecco's phosphate buffered saline (PBS), pH 7.4, at 4 °C with a IKA®Ultra-Turrax® T25 Digital Homogenizer (for 60 s). The homogenate was centrifuged at 5000 rpm for 10 min and the surnatant was used for the assay. 15 μL of 5 mM stock solutions of compounds **14**–**15** in DMSO

were added to 1.485 mL of the cytosolic preparation thus incubating final compounds concentration equal to 50 μM.

Samples were kept in the dark under gentle stirring (not in the case of human serum and cytosolic fractions) and incubated at 37 ± 0.5 °C. At appropriate time intervals, aliquots (100 μL) were diluted or deproteinized with methanol or acetonitrile (400 μL) before injection. In the case of serum and cytosolic suspensions, after the addition of methanol the samples were vortexed for 1 min and centrifuged at 3500 rpm for 5 min and the supernatant was filtered and injected. Samples were analyzed by HPLC using a Kinetex-C18 (2.1 mm × 150 mm, with 2.6 μm size particles, 100 Å) on an Analytic Agilent 1260 Infinity multidetector system equipped with a 1200 series UV-diode array detector. UV spectra were recorded at 320 nm. Analytes were eluted in isocratic conditions by using mixtures of acetonitrile and ammonium formate buffer (20 mM, pH 5.00) as the mobile phase. The mobile phase was filtered through a Nylon-66 membrane 0.45 μm (Supelco, USA) before use. Injection volumes were 2 μL and the flow rate was 0.2 mL/min. Data were integrated and reported using OpenLAB software (Agilent Technologies).

Calibration lines for alcohols **9d**, **11** and **12a** were obtained by injecting 1 μL of different stock solutions (1–200 μM in methanol containing 10% DMSO, v/v) after dilution with cold methanol (100 μL–500 μL) and measuring the peak area absorbance at 320 nm. Percentage of conversion was calculated by using the following equation:

$$\% \text{ conversion} = (c_t/c_{max}) \times 100$$

where c_t was the concentration measured at time t and c_{max} represents the maximal concentration (equal to the initial concentration of **14**–**16** in the incubated samples at t_0). Each kinetic experiment was performed in triplicate. Linear and non-linear regression analyses were performed with Prism 5.0. Data are the mean ± SD.

6.5. Cytotoxicity assays and neuroprotection against oxidative stress insults

Cytotoxicity assays were carried out against human neuroblastoma cell line SH-SY5Y as previously described [60]. Cells were maintained at 37 °C in a humidified incubator containing 5% CO_2 in DMEM (EuroClone) nutrient supplemented with 10% heat inactivated FBS (EuroClone), 2 mM L-glutamine (EuroClone), 100 U/mL penicillin and 100 μg/mL streptomycin (EuroClone). Cytotoxicity of compounds is expressed as IC_{50} values, the concentrations that cause 50% growth inhibition. The results were determined using the 3-(4,5-dimethylthiazol-2-yl)-2,5-diphenyl-tetrazolium bromide (MTT) assay. Cells were dispensed into 96-well microtiter plates at a density of 5000 cells/well. Following overnight incubation, cells were treated with the compounds in the range concentration 0.01–100 μM. Then the plates were incubated at 37 °C for 24 h. An amount of 10 μL of MTT (0.5% w/v) was further added to each well and the plates were incubated for an additional 2 h at 37 °C. Finally, the blue formazan crystals were dissolved by addition of 100 μL of DMSO. Absorbance at 570 nm was determined using a Perkin Elmer 2030 multilabel reader Victor TM X3.

The oxidative stress in the same neuroblastoma lines was reproduced by incubating cells rotenone (20 μM) as specific mitochondrial insult [61] or hydrogen peroxide (200 μM) as a non selective reactive species [62]. To study the neuroprotective action of compounds **9d**, **12a**, **14**, **15** and donepezil against the inhibition of cell proliferation induced by rotenone and H_2O_2, SH-SY5Y cells were pre-incubated for 24 h with compounds at concentrations 0.1, 0.5 and 2.5 μM, then the media was replaced with the media containing the combination of compounds plus the insults and incubated for further 24 h [48]. Cell proliferation was assessed by MTT assay and data are expressed as the percentage of viable cells referred to cells incubated without insults and compounds (control). Each compound was tested in triplicate. Standard error of the mean (SD) is given. Statistical significance was determined using a two-way analysis of variance (ANOVA) followed by the Bonferroni post hoc tests (GraphPad Prism version 5) and was assigned to $p < 0.01$ (**) and $p < 0.001$ (***).

6.6. Bidirectional transport studies on MDCKII-MDR1 monolayers

The bi-directional transport studies were conducted as previously described by using Madin-Darby Canine Kidney (MDCK) cells retrovirally transfected with the human MDR1 cDNA (MDCKII-MDR1) as a blood-brain barrier penetration model [63]. The flux of fluorescein isothiocyanate-dextran (FD4, Sigma-Aldrich, Italy) and diazepam was used to verify cell barrier function and integrity. The analysis of compounds **9d**, **12a**, **14**–**15** was performed through UV−visible spectroscopy using a PerkinElmer double-beam UV−visible spectrophotometer Lambda Bio 20 (Milan, Italy), equipped with 10 mm path-length-matched quartz cells. Standard calibration curves were prepared at maximum absorption wavelength of each compound using PBS as solvent and were linear ($r^2 = 0.999$) over the range of tested concentration (from 5 to 75 μM). The FD4 samples were analyzed with a Victor3 fluorimeter (Wallac Victor3, 1420 Multilabel Counter, PerkinElmer) at excitation and emission wavelengths of 485 and 535 nm, respectively. Each compound was tested in triplicate, and the experiments were repeated three times. Data are reported as the apparent permeability (P_{app}), calculated in units of cm/s [28]. The efflux ratio (ER) was calculated using the following equation: ER = P_{app}, BL/P_{app}, AP where P_{app}, AP is the apparent permeability of apical-to-basal transport expressed in cm/sec and P_{app}, BL is the apparent permeability of basal-to-apical transport expressed in cm/sec. An ER greater than 2 indicates that a test compound is likely to be a substrate for P-gp transport.

Notes

The authors declare no competing financial interest.

Author contributions

L.P. designed the project, carried out the synthesis and stability studies, wrote the paper. R.M.I. performed the cell-based assays and revised the paper. M.C. carried out the in vitro screening and supervised the project. M.R. and R.F. contributed to the synthesis. N.D. analyzed and supervised cell-based experiments. S.C. analyzed and supervised the stability studies. C.D.A. supervised the project and contributed to write the paper. All authors have given approval to the final version of the manuscript.

Funding sources

L.P. acknowledges financial support from APQ Research Apulian Region "FutureInResearch (FKY7YJ5) - Regional program for smart specialization and social and environmental sustainability" Fondo di Sviluppo e Coesione 2007–2013.

Acknowledgment

The authors thank Prof. A. Carotti for helpful discussions and A. Palermo for technical assistance in NMR experiments.

Appendix A. Supplementary data

Supplementary data to this article can be found online at https://doi.org/10.1016/j.ejmech.2018.10.016.

References

[1] H.W. Querfurth, F.M. LaFerla, Alzheimer's disease, N. Engl. J. Med. 362 (2010) 329–344.
[2] W.V. Graham, A. Bonito-Oliva, T.P. Sakmar, Update on Alzheimer's disease therapy and prevention strategies, Annu. Rev. Med. 68 (2017) 413–430.
[3] J.L. Cummings, T. Morstorf, K. Zhong, Alzheimer's disease drug-development pipeline: few candidates, frequent failures, Alzheimer's Res. Ther. 6 (2014) 37–43.
[4] R. Anand, K.D. Gill, A.A. Mahdi, Alzheimer's disease: targeting the cholinergic system, Neuropharmacology 76 (2014) 27–50.
[5] A.V. Terry Jr., J.J. Buccafusco, The cholinergic hypothesis of age and Alzheimer's disease-related cognitive deficits: recent challenges and their implications for novel drug development, J. Pharmacol. Exp. Therapeut. 306 (2003) 821–827.
[6] E. Giacobini, Cholinesterase inhibitors stabilize Alzheimer's disease, Neurochem. Res. 25 (2000) 1185–1190.
[7] E. Scarpini, P. Scheltens, H. Feldman, Treatment of Alzheimer's disease: current status and new perspectives, Lancet Neurol. 2 (2003) 539–547.
[8] W.J. Deardorff, E. Feen, G.T. Grossberg, The use of cholinesterase inhibitors across all stages of Alzheimer's disease, Drugs Aging 32 (2015) 537–547.
[9] J.A. Hardy, G.A. Higgins, Alzheimer's disease: the amyloid cascade hypothesis, Science 256 (1992) 184–185.
[10] K. Blennow, N. Mattsson, M. Schöll, O. Hansson, H. Zetterberg, Amyloid biomarkers in Alzheimer's disease, Trends Pharmacol. Sci. 36 (2015) 297–309.
[11] J. Hardy, D.J. Selkoe, The amyloid hypothesis of Alzheimer's disease: progress and problems on the road to therapeutics, Science 297 (2002) 353–356.
[12] M. Rosini, E. Simoni, A. Milelli, A. Minarini, C. Melchiorre, Oxidative stress in Alzheimer's disease: are we connecting the dots?, J. Med. Chem. 57 (2014) 2821–2831.
[13] M.A. Smith, C.A. Rottkamp, A. Nunomura, A.K. Raina, G. Perry, Oxidative stress in Alzheimer's disease, Biochim. Biophys. Acta 1502 (2000) 139–144.
[14] S. Ayton, P. Lei, A.I. Bush, Metallostasis in Alzheimer's disease, Free Radic. Biol. Med. 62 (2013) 76–89.
[15] G.J. Biessels, S. Staekenborg, E. Brunner, C. Brayne, P. Scheltens, Risk of dementia in diabetes mellitus: a systematic review, Lancet Neurol. 5 (2006) 64–74.
[16] C.-C. Liu, T. Kanekiyo, H. Xu, G. Bu, Apolipoprotein E and Alzheimer disease: risk, mechanisms, and therapy, Nat. Rev. Neurol. 9 (2013) 106–118.
[17] R. Morphy, C. Kay, Z. Rankovic, From magic bullets to designed multiple ligands, Drug Discov. Today 9 (2004) 641–651.
[18] A. Cavalli, M.L. Bolognesi, A. Minarini, M. Rosini, V. Tumiatti, M. Recanatini, C. Melchiorre, Multi-target-directed ligands to combat neurodegenerative diseases, J. Med. Chem. 51 (2008) 347–372.
[19] R. Leon, A.G. Garcia, J. Marco-Contelles, Recent advances in the multitarget-directed ligands approach for the treatment of Alzheimer's disease, Med. Res. Rev. 33 (2013) 139–189.
[20] S.L. Greig, Memantine ER/Donepezil: a review in Alzheimer's disease, CNS Drugs 29 (2015) 963–970.
[21] L. Pisani, R. Farina, R. Soto-Otero, N. Denora, G.F. Mangiatordi, O. Nicolotti, E. Mendez-Alvarez, C.D. Altomare, M. Catto, A. Carotti, Searching for multi-targeting neurotherapeutics against Alzheimer's: discovery of potent AChE-MAO B inhibitors through the decoration of the 2H-Chromen-2-one structural motif, Molecules 21 (2016) 362–376.
[22] J. Marco-Contelles, M. Unzeta, I. Bolea, G. Esteban, R.R. Ramsay, A. Romero, R. Martínez-Murillo, M.C. Carreiras, L. Ismaili, ASS234, as a new multi-target directed propargylamine for Alzheimer's disease therapy, Front. Neurosci. 10 (2016) 294–300.
[23] J. Sterling, Y. Herzig, T. Goren, N. Finkelstein, D. Lerner, W. Goldenberg, I. Miskolczi, S. Molnar, F. Rantal, T. Tamas, G. Toth, A. Zagyva, A. Zekany, J. Finberg, G. Lavian, A. Gross, R. Friedman, M. Razin, W. Huang, B. Krais, M. Chorev, M.B. Youdim, M. Weinstock, Novel dual inhibitors of AChE and MAO derived from hydroxy aminoindan and phenethylamine as potential treatment for Alzheimer's disease, J. Med. Chem. 45 (2002) 5260–5279.
[24] J. Joubert, G.B. Foka, B.P. Repsold, D.W. Oliver, E. Kapp, S.F. Malan, Synthesis and evaluation of 7-substituted coumarin derivatives as multimodal monoamine oxidase-B and cholinesterase inhibitors for the treatment of Alzheimer's disease, Eur. J. Med. Chem. 125 (2017) 853–864.
[25] S.-S. Xie, J.-S. Lan, X. Wang, Z.-M. Wang, N. Jiang, F. Li, J.-J. Wu, J. Wang, L.-Y. Kong, Design, synthesis and biological evaluation of novel donepezil–coumarin hybrids as multi-target agents for the treatment of Alzheimer's disease, Bioorg. Med. Chem. 24 (2016) 1528–1539.
[26] J. Saura, J.M. Luque, A.M. Cesura, M. Da Prada, V. Chan-Palay, G. Huber, J. Löffler, J.G. Richards, Increased monoamine oxidase B activity in plaque-associated astrocytes of Alzheimer Brains revealed by quantitative enzyme radioautography, Neuroscience 62 (1994) 15–30.
[27] R. Farina, L. Pisani, M. Catto, O. Nicolotti, D. Gadaleta, N. Denora, R. Soto-Otero, E. Mendez-Alvarez, C.S. Passos, G. Muncipinto, C.D. Altomare, A. Nurisso, P.A. Carrupt, A. Carotti, Structure-based design and optimization of multitarget-directed 2H-chromen-2-one derivatives as potent inhibitors of monoamine oxidase B and cholinesterases, J. Med. Chem. 58 (2015) 5561–5578.
[28] L. Pisani, R. Farina, M. Catto, R.M. Iacobazzi, O. Nicolotti, S. Cellamare, G.F. Mangiatordi, N. Denora, R. Soto-Otero, L. Siragusa, C.D. Altomare, A. Carotti, Exploring basic tail modifications of coumarin-based dual acetylcholinesterase-monoamine Oxidase B inhibitors: identification of water-soluble, brain-permeant neuroprotective multitarget agents, J. Med. Chem. 59 (2016) 6791–6806.
[29] V. Calabrese, C. Mancuso, M. Calvani, E. Rizzarelli, D.A. Butterfield, A.M.G. Stella, Nitric oxide in the central nervous system: neuroprotection versus neurotoxicity, Nat. Rev. Neurosci. 8 (2007) 766–775.
[30] P.G. Wang, M. Xian, X. Tang, X. Wu, Z. Wen, T. Cai, A.J. Janczuk, Nitric oxide donors: chemical activities and biological applications, Chem. Rev. 102 (2002) 1091–1134.
[31] B. Rolando, L. Lazzarato, M. Donnola, E. Marini, S. Joseph, G. Morini, C. Pozzoli, R. Fruttero, A. Gasco, Water-soluble nitric-oxide-releasing acetylsalicylic acid (ASA) prodrugs, ChemMedChem 8 (2013) 1199–1209.
[32] L.L. Fershtat, N.N. Makhova, Molecular hybridization tools in the development of furoxan-based NO-donor prodrugs, ChemMedChem 12 (2017) 622–638.
[33] B. Testa, J.M. Mayer, The cleavage of esters of inorganic acids, in: T. Kolitzus, P.L. Bounds (Eds.), Hydrolysis in Drug and Prodrug Metabolism: Chemistry, Biochemistry, and Enzymology, Verlag Helvetica Chimica Acta AG: Zurich; WILEY-VCH GmbH & Co. KGaA, Weineim, 2003, pp. 535–590.
[34] H. Dvira, I. Silman, M. Harel, T.L. Rosenberry, J.L. Sussman, Acetylcholinesterase: from 3D structure to function, Chem. Biol. Interact. 187 (2010) 10–22.
[35] J. Cheung, M.J. Rudolph, F. Burshteyn, M.S. Cassidy, E.N. Gary, J. Love, M.C. Franklin, J.J. Height, Structures of human acetylcholinesterase in complex with pharmacologically important ligands, J. Med. Chem. 55 (2012) 10282–10286.
[36] D.M. Wong, H.M. Greenblatt, H. Dvir, P.R. Carlier, Y.-F. Han, Y.-P. Pang, I. Silman, J.L. Sussman, Acetylcholinesterase complexed with bivalent ligands related to huperzine A: experimental evidence for species-dependent protein-ligand complementarity, J. Am. Chem. Soc. 125 (2003) 363–373.
[37] C. Binda, P. Newton-Vinson, F. Hubalek, D.E. Edmondson, A. Mattevi, Structure of human monoamine oxidase B, a drug target for the treatment of neurological disorders, Nat. Struct. Mol. Biol. 9 (2002) 22–26.
[38] L. Pisani, R. Farina, O. Nicolotti, D. Gadaleta, R. Soto-Otero, M. Catto, M. Di Braccio, E. Mendez-Alvarez, A. Carotti, In silico design of novel 2H-chromen-2-one derivatives as potent and selective MAO-B inhibitors, Eur. J. Med. Chem. 89 (2015) 98–105.
[39] L. Fang, D. Appenroth, M. Decker, M. Kiehntopf, C. Roegler, T. Deufel, C. Fleck, S. Peng, Y. Zhang, J. Lehmann, Synthesis and biological evaluation of NO-donor-tacrine hybrids as hepatoprotective anti-Alzheimer drug candidates, J. Med. Chem. 51 (2008) 713–716.
[40] G.L. Ellman, K.D. Courtney, V. Andres Jr., R.M. Feartherstone, A new and rapid colorimetric determination of acetylcholinesterase activity, Biochem. Pharmacol. 7 (1961) 88–95.
[41] F. Denizot, R. Lang, Rapid colorimetric assay for cell growth and survival. Modifications to the tetrazolium dye procedure giving improved sensitivity and reliability, J. Immunol. Methods 89 (1986) 271–277.
[42] J.P. Finberg, K. Gillman, Selective inhibitors of monoamine oxidase type B and the "cheese effect", Int. Rev. Neurobiol. 100 (2011) 169–190.
[43] P. Riederer, W. Danielczyk, E. Gruenblatt, Monoamine oxidase-B inhibition in Alzheimer's disease, Neurotoxicology 1 (2004) 271–277.
[44] M.-M. Mesulam, C. Geula, Butyrylcholinesterase reactivity differentiates the amyloid plaques of aging from those of dementia, Ann. Neurol. 36 (1994) 722–727.
[45] M. Mesulam, A. Guillozet, P. Shaw, B. Quinn, Widely spread butyrylcholinesterase can hydrolyze acetylcholine in the normal and Alzheimer brain, Neurobiol. Dis. 9 (2002) 88–93.
[46] S. Darvesh, M.K. Cash, G.A. Reid, E. Martin, A. Mitnitski, C. Geula, Butyrylcholinesterase is associated with β-amyloid plaques in the transgenic APPSWE/PSEN1dE9 mouse model of Alzheimer disease, J. Neuropathol. Exp. Neurol. 71 (2012) 2–14.
[47] G. Sorba, C. Medana, R. Fruttero, C. Cena, A. Di Stilo, U. Galli, A. Gasco, Water soluble furoxan derivatives as NO prodrugs, J. Med. Chem. 40 (1997) 463–469.
[48] M. Benchekroun, M. Bartolini, J. Egea, A. Romero, E. Soriano, M. Pudlo, V. Luzet, V. Andrisano, M.L. Jimeno, M.G. López, S. Wehle, T. Gharbi, B. Refouvelet, L. de Andrés, C. Herrera-Arozamena, B. Monti, M.L. Bolognesi, M.I.

Rodríguez-Franco, M. Decker, J. Marco-Contelles, L. Ismaili, Novel tacrine-grafted Ugi adducts as multipotent anti-Alzheimer drugs: a synthetic renewal in tacrine–ferulic acid hybrids, ChemMedChem 10 (2015) 523–539.
[49] Z. Rankovic, CNS drug design: balancing physicochemical properties for optimal brain exposure, J. Med. Chem. 58 (2015) 2584–2608.
[50] H. von Pechmann, C. Duisberg, Ueber die verbindungen der phenole mit acetessigäther, Ber. Dtsch. Chem. Ges. 16 (1883) 2119–2128.
[51] O. Gia, E. Uriarte, G. Zagotto, F. Baccichetti, C. Antonello, S. Marciani-Magno, Synthesis and photobiological activity of new methylpsoralen derivatives, J. Photochem. Photobiol., B 14 (1992) 95–104.
[52] C. Gnerre, M. Catto, F. Leonetti, P. Weber, P.-A. Carrupt, C. Altomare, A. Carotti, B. Testa, Inhibition of monoamine oxidases by functionalized coumarin derivatives: biological activities, QSARs, and 3D-QSARs, J. Med. Chem. 43 (2000) 4747–4758.
[53] L. Pisani, M. Barletta, R. Soto-Otero, O. Nicolotti, E. Mendez-Alvarez, M. Catto, A. Introcaso, A. Stefanachi, S. Cellamare, C. Altomare, A. Carotti, Discovery, biological evaluation, and structure−activity and −selectivity relationships of 6′-substituted (E)-2-(benzofuran-3(2H)-ylidene)-N-methylacetamides, a novel class of potent and selective monoamine oxidase inhibitors, J. Med. Chem. 56 (2013) 2651–2664.
[54] M.C. Breschi, V. Calderone, M. Digiacomo, M. Macchia, A. Martelli, E. Martinotti, F. Minutolo, S. Rapposelli, A. Rossello, L. Testai, A. Balsamo, New NO-releasing pharmacodynamic hybrids of losartan and its active metabolite: design, synthesis, and biopharmacological properties, J. Med. Chem. 49 (2006) 2628–2639.
[55] L. Pisani, M. Catto, A. De Palma, R. Farina, S. Cellamare, C.D. Altomare, Discovery of potent dual binding site acetylcholinesterase inhibitors via homo- and heterodimerization of coumarin-based moieties, ChemMedChem 12 (2017) 1349–1358.
[56] L. Pisani, M. Catto, O. Nicolotti, G. Grossi, M. Di Braccio, R. Soto-Otero, E. Mendez-Alvarez, A. Stefanachi, D. Gadaleta, A. Carotti, Fine molecular tuning at position 4 of 2H-chromen-2-one derivatives in the search of potent and selective monoamine oxidase B inhibitors, Eur. J. Med. Chem. 70 (2013) 723–739.
[57] L. Pisani, M. Rullo, M. Catto, M. de Candia, A. Carrieri, S. Cellamare, C.D. Altomare, Structure–property relationship study of the HPLC enantioselective retention of neuroprotective 7-[(1-alkylpiperidin-3-yl)methoxy]coumarin derivatives on an amylose-based chiral stationary phase, J. Separ. Sci. 41 (2018) 1376–1384.
[58] A. Conejo-García, L. Pisani, M. d. C. Núñez, M. Catto, O. Nicolotti, F. Leonetti, J.M. Campos, M.A. Gallo, A. Espinosa, A. Carotti, Homodimeric bis-quaternary heterocyclic ammonium salts as potent acetyl- and butyryl-cholinesterase inhibitors: a systematic investigation of the influence of linker and cationic heads over affinity and selectivity, J. Med. Chem. 54 (2011) 2627–2645.
[59] L. Pisani, A. De Palma, N. Giangregorio, D.V. Miniero, P. Pesce, O. Nicolotti, F. Campagna, C.D. Altomare, M. Catto, Mannich base approach to 5-methoxyisatin 3-(4-Isopropylphenyl)hydrazone: a water-soluble prodrug for a multitarget inhibition of cholinesterases, beta-amyloid fibrillization and oligomer-induced cytotoxicity, Eur. J. Pharmaceut. Sci. 109 (2017) 381–388.
[60] R.M. Iacobazzi, L. Porcelli, A.A. Lopedota, V. Laquintana, A. Lopalco, A. Cutrignelli, E. Altamura, R. Di Fonte, A. Azzariti, M. Franco, N. Denora, Targeting human liver cancer cells with lactobionic acid-G(4)-PAMAM-FITC sorafenib loaded dendrimers, Int. J. Pharm. 528 (2017) 485–497.
[61] N. Li, K. Ragheb, G. Lawler, J. Sturgis, B. Rajwa, A.J. Melendez, J.P. Robinson, Mitochondrial complex I inhibitor rotenone induces apoptosis through enhancing mitochondrial reactive oxygen species production, J. Biol. Chem. 278 (2003) 8516–8525.
[62] I. Sipos, L. Tretter, V. Adam-Vizi, Quantitative relationship between inhibition of respiratory complexes and formation of reactive oxygen species in isolated nerve terminals, J. Neurochem. 84 (2003) 112–118.
[63] N. Denora, V. Laquintana, A. Lopedota, M. Serra, L. Dazzi, G. Biggio, D. Pal, A.K. Mitra, A. Latrofa, G. Trapani, G. Liso, Novel L-dopa and dopamine prodrugs containing a 2-phenyl-imidazopyridine moiety, Pharm. Res. (N. Y.) 24 (2007) 1309–1324.